Long Range Acoustic Communication Based on Optimal Waveform Design

FINAL REPORT

Woods Hole Oceanographic Institution

Woods Hole, MA 02543-1047

September 1997

Submitted To:

The Defense Advanced Research Projects Agency
in fulfillment of Contract MDA972-95-1-0006

TABLE OF CONTENTS

Phase-Coherent Equalization Methods for Complex Underwater Acoustic Communication Channels

Lee Freitag
Woods Hole Oceanographic Institution

Introduction

Acoustic communications for long-range underwater applications is made difficult by a number of environmental factors. The most important of these in shallow-water propagation is the effect of the large number of ray paths that are observed after the sound travels from the source to the receiver. The summation of these rays at the receiver causes constructive and destructive interference, resulting in spectral shaping that varies over both time and space. The time spread of the channel, which can range from several milliseconds to a large fraction of a second, is the most difficult effect to overcome as the range from the source to the receiver increases. However, not only does the delay spread continues to increase as range increases but the signal to noise ratio drops as well, making what is already a challenging channel even more difficult. In addition, when source and receiver are in motion, Doppler shifts are present, moving the center frequency of the signal and warping it in time. Doppler shift is present not only due to the gross movement of the source and receiver, but is also added to each ray as it grazes a moving reflector such as the ocean's surface. While numerous other obstacles exist (for example, man-made and biologic noise), delay spread continues to dominate the list of problems for underwater communication. The problem will only continue to worsen as source levels are increased in an attempt to increase range, which has the effect of lengthening the overall impulse response and increasing the number of turns or bounces each ray has experienced.

A key question regarding acoustic communication is this: What is the most effective method for signaling over this channel at the highest possible rate at the farthest possible range? While this is a difficult question, it can be simplified by making some assumptions. One, for a fixed bandwidth and a desire to maximize transmission rate, on a channel with unknown spectral nulls it makes sense to utilize all of the frequency band all of the time, adding redundancy in coding and processing that exploits all available degrees of freedom. A phase-coherent system with symbol rate selected to utilize all the available bandwidth, combined with the appropriate multi-channel receiver, is appropriate for operation under these types of conditions, provided that the receive algorithm is capable of compensating for the channel effects noted above. It is acknowledged that when absolute reliability at the maximum range is required then other methods should be considered, particularly those that provide one or two orders of magnitude more energy per bit.

However, given that a phase-coherent system is optimal for maximizing throughput, one can focus on development of the receiver algorithm. In this paper the shallow-water channel is first examined and found to have significant time spread over a narrow spread of arrival angles. Next the equalization algorithm is discussed, in particular, aspects which are important for the complex long-range shallow-water channel.

Specific topics to be discussed include:

- Single channel and multi-channel phase-locked loops and the effect of PLL gain upon performance.
- The recursive least-squares (RLS) adaptive filter algorithm and the impact of tracking rate settings upon performance. Four case studies are presented to demonstrate that different acoustic channels require different tracking rates in order to achieve optimal performance.
- Within the section on optimal tracking rate the effect of changing the number of parameters used in the equalizer is presented and the impact of correct parameterization discussed.
- An *adaptive* tracking rate version of the RLS algorithm is presented as an answer to the issue of optimal settings of the tracking rate, though at a high computational cost.
- An *adaptive* step-size least mean square (LMS) algorithm is discussed as a compromise between self-optimization and reasonable computational complexity.
- Lastly, the acoustic channels shown in the motivation section are equalized and the results are presented. As part of this discussion an example of how the equalizer performs automatic beamforming as part of the feedforward filtering is shown.

It should be noted that despite the stated goal of effectively operating on very complex acoustic channels, the algorithm which will equalize the complex channels will also work on simpler channels. It is, however, desired that the computational complexity of the receiver be adaptively reduced as appropriate for decoding data from the simpler channel. An example of such a channel is single convergence-zone propagation at 2-5 kHz. Depending on source-receiver depths there may only be a few ray paths to the receiver, and while the SNR is often low, the low complexity should greatly simplify equalization. Indeed, the receiver presented in this paper has the property of reducing computational complexity adaptively whenever possible.

Acknowledgments

A portion of the work presented here was done in collaboration with Mark Johnson and Milica Stojanovic and reported in [5] and [6]. Work from those papers is noted by reference in the text.

The continental shelf data presented here is from a test performed off the coast of New England in 1996 and funded by ONR through Sanders-Lockheed-Martin.

Some of the data used in the section on optimal forgetting-factor analysis was collected in 1995 offshore Ft. Lauderdale and funded by DARPA under contract MDA972-95-1-005 as part of the AMMT program.

This work was supported by DARPA under contract MDA972-95-0006.

The Long-Range Shallow-Water Channel: Time Spread

In propagation on and near the continental-shelf where water depths are less than 200 meters time spreads of 20 to 100 msec are common. This translates into 25 to 120 symbol durations when data is transmitted at 1200 symbols per second. In term of symbol span, this period is much longer than many other conventional data communication channels. Examples of these channels, observed during an experiment near the edge of the New England continental shelf in August 1996, are shown in Figs. 1-4 on the following pages. The data were collected using an array with 1m element spacing located at about 70 m depth in about 100 m of water. The center frequency of the transmissions is 2.25 kHz and 1250 Hz of bandwidth was used. During most of the experiment the receiver was drifting very slowly (less than half a knot), while the vessel towing the source steamed away at 2-3 knots.

In Fig. 1 a relatively close-range impulse response is shown. Taken at range of 3.5 miles (6.4 km) it contains a group of initial arrivals spanning about 20 msec followed by lower-amplitude sparse arrivals with a total span of about 100 msec. While a very small signal is present about 150 msec after the first arrival, its amplitude is quite low. These later ($t>0.15$ s) arrivals disappear slowly as range increases, and as they disappear the first 40-50 msec after the initial arrival begins to become increasingly populated with additional rays as shown in Fig. 2.

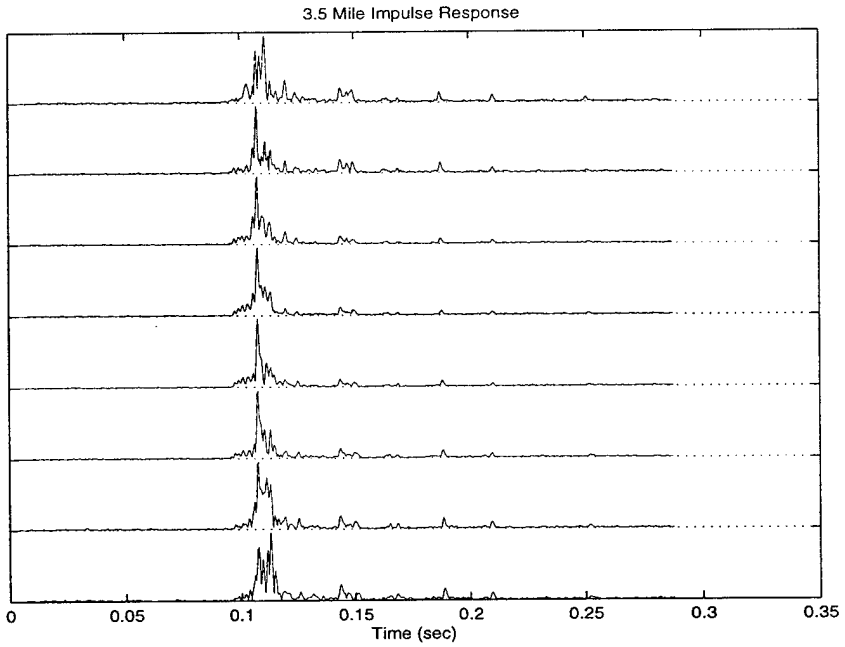

Fig. 1. The close-range shallow-water channel showing both moderate spread in the initial arrival set and a number of later, discrete arrivals. The hydrophones are 1 m apart located 70 m deep in about 100 m water.

The impulse response of Fig. 2 is taken at 16 miles (29 km) and it shows a well-developed channel with many arrivals of similar amplitude over the 40 msec time spread. While the location of the peak is similar on the first 6 channels, on the last two it shifts to a point about 20 msec later. This demonstrates some of the spatial variability of the channel. Proceeding to 24 miles (about 44 km) as shown in Fig. 3, the channel is slightly longer but fairly similar to that at 16 miles (though plotted to show more detail of the arrival structure). While the overall envelope of the multipath increases slowly, the pattern of arrivals within the group is variable from packet to packet and hydrophone to hydrophone. While any given pair of hydrophones share similar features, non-adjacent hydrophones are often quite dissimilar.

While the time duration of the channel is long relative to the symbol rate, there are two reasons to believe that the data will be decodable: (1) The SNR is quite high, and (2) the spatial variability across the array is high which means that some diversity gain should be available through the use of the multi-channel receiver.

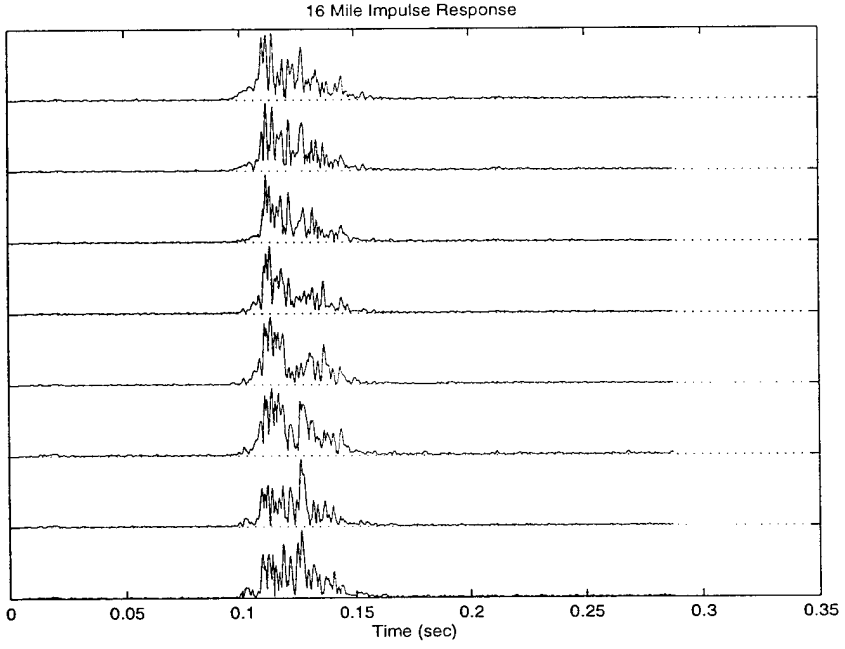

Fig. 2. At 16 miles the later arrivals are gone and the initial arrival group has more spread and somewhat larger spatial variability than that observed at 3.5 miles.

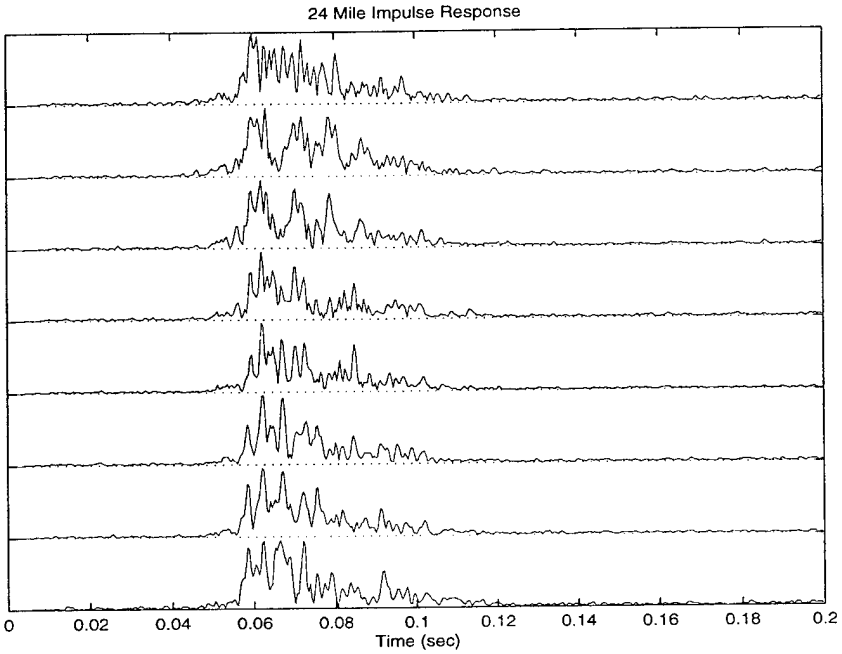

Fig. 3. At 24 miles channel spread has increased slightly over that observed at 16 miles. The arrival energy is well-spread over time and one may observe that on some hydrophones there are rays present that do not exist on adjacent hydrophones. For example, the 3rd 'hump' of peaks on channel 3 is not present on channel 4.

While the channels shown in Fig. 1-3 appear quite challenging for coherent communication, these impulse responses appear simple in comparison with that shown in Fig. 4. Here the range is only 11 miles, but the bathymetry and sound-speed are such that a very complex channel is created. The time spread is over 100 msec and the arrival structure appears incoherent (at least to the eye) from hydrophone to hydrophone. Not only is the delay spread large, the arrivals slowly increase in amplitude between t=0.06 and t=0.08, providing an indeterminate start point and, as well, an acausal channel. The spectra of this channel is quite variable (see Fig. 5 in Appendix B for a similar channel).

Unfortunately, this channel cannot be dismissed as one that is unusual or not of interest: communication over areas of disparate bathymetry is important for many practical applications (for example, an offshore vessel transmitting to a UUV in shallower water). Thus an equalizer with the capability to operate on such long channels is required when deploying acoustic modems in these types of environments. It should be noted that the bathymetric differences cause only a portion of the problem, the different sound speed profiles that are present through the shelf transition are also important in creating this arrival structure. While the task of equalizing the channel shown in Fig. 4 as a laboratory analysis task is daunting enough, due to the fact that this channel could be observed by a UUV, it must be equalizable using finite computational resources in near real-time without operator intervention.

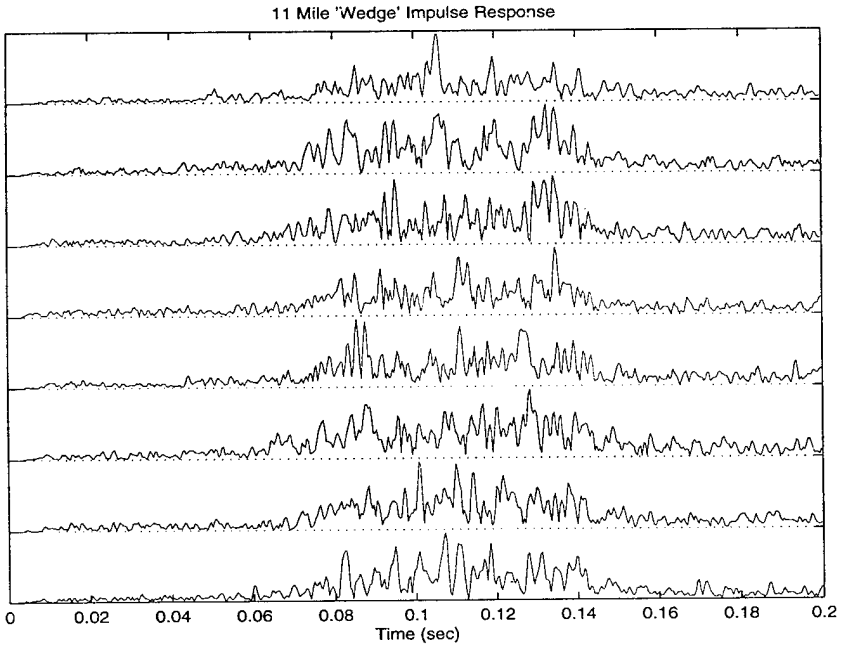

Fig. 4. Impulse response for up-slope propagation ('wedge') at moderate range.

The Long-Range Shallow-Water Channel: Angle of Arrival

The multichannel receiver algorithm is a space-time processor which acts effectively as a beamformer as well as an equalizer. Thus when arrivals at the array are separated in angle, the signal is enhanced by coherently focussing on the strongest ray and suppressing others. This is one of the key strengths of the receiver described in the following sections. The feedforward filter coefficients are automatically adapted in order to minimize the output error, which in turn will steer the main beam of the array toward one incoming ray and as well attempt to null other, interfering rays. An example of how this works is included in the results section.

For the shallow-water channel the angle of arrival at the array is always quite small. A modeling run done using data taken before the 1996 experiment indicated that the arrival angles would not exceed about +/- 13 degrees (Fig. 5).

Actual measurements of arrival angle using short-baseline direction-of-arrival techniques on several hydrophones demonstrates similar angle of arrival ranges, though the details of the arrival structure are different.

This narrow spread in angular arrivals makes it difficult to employ standard beamformers that are not adaptive and capable of steering nulls at other interfering arrivals. For the (relatively) small apertures under consideration with practical arrays the main beam width is large enough to include most of the energy shown below. Thus the importance of the adaptive beamforming capability of the equalizer.

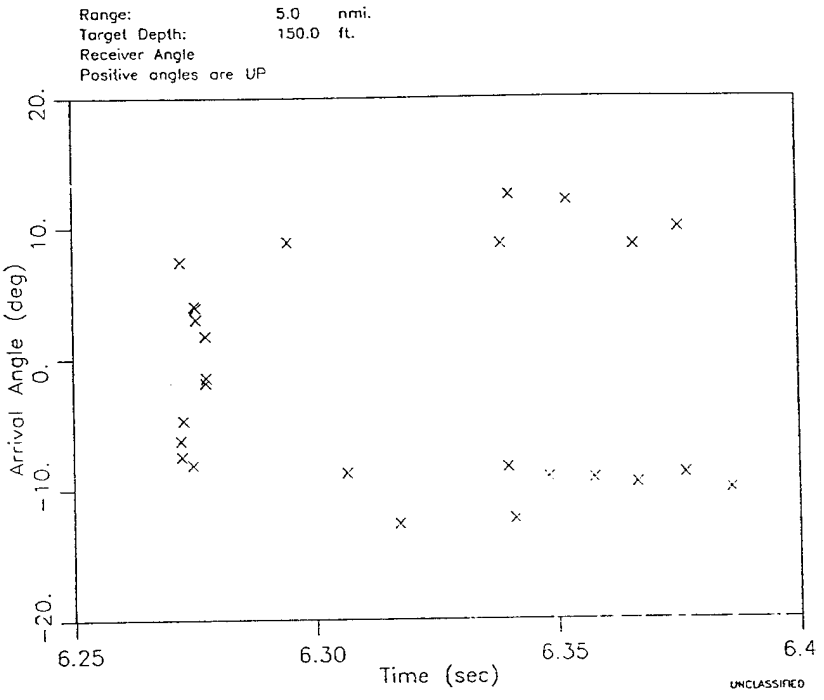

Fig. 5. Example of model output with angle of arrival estimates for a number of eigenrays. The model was run using data taken just before the New England Continental Shelf experiment in 1996.

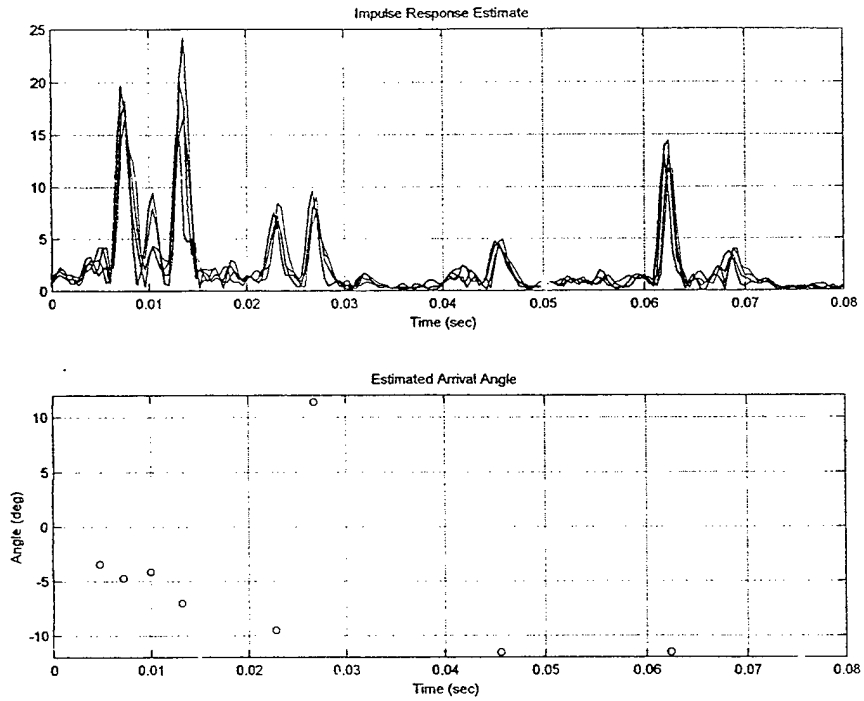

Fig. 6. Impulse response and angle of arrival estimate at close-range (about 3 miles).

The purpose of the remainder of this report is to explore the equalization of complex channels with robust methods that are computationally efficient and amenable to implementation on completely embedded systems operating in autonomous situations or used on manned vessels without the need for a specialist.

Decision Feedback Equalizer Receiver Structure

The multichannel decision-feedback equalizer (DFE) utilizing the recursive least-squares (RLS) parameter update was introduced for underwater acoustics in [2] and recently augmented with Doppler pre-processing in [5]. Leaving aside the pre-processing aspects of the algorithm for the moment, the basic structure of the equalizer is shown in the figure below. There are m fractionally-spaced (T/2) feedforward filters, one for each hydrophone input, all of which are combined with the feedback filter output prior to phase correction via a 2nd order phase-locked loop (PLL). The output symbol decision is fed back under the assumption that it is correct and the error signal is provided to the adaptation algorithm for the next parameter update. The adaptation algorithm may be any one of a number of adaptive filters, chosen to balance complexity and performance. In order to maximize efficiency, the parameter update is only performed when the mean-square error exceeds a certain value [8]. This is termed sparse updating.

Regardless of which adaptive filter is used, the algorithm requires that a number of settings be determined in advance in order to ensure good performance. The more difficult the acoustic channel, the more important it is to choose these settings appropriately. For example, a simple, high-SNR channel can be equalized over a large range of parameter settings (though not necessarily to the optimal performance level), whereas for a low-SNR time-varying channel, zero-error performance may only be attained over a tiny parameter set whose values must be selected through trial and error.

The goal of the current receiver design is to not only equalize extremely complex channels, but to remove, wherever possible, critical dependence upon carefully chosen parameters that must be manually changed as the acoustic channel varies. The objective is, instead, to offer good performance over a wide a range of settings and channels. The system would thus be robust with respect to both channel changes and small variations in the settings.

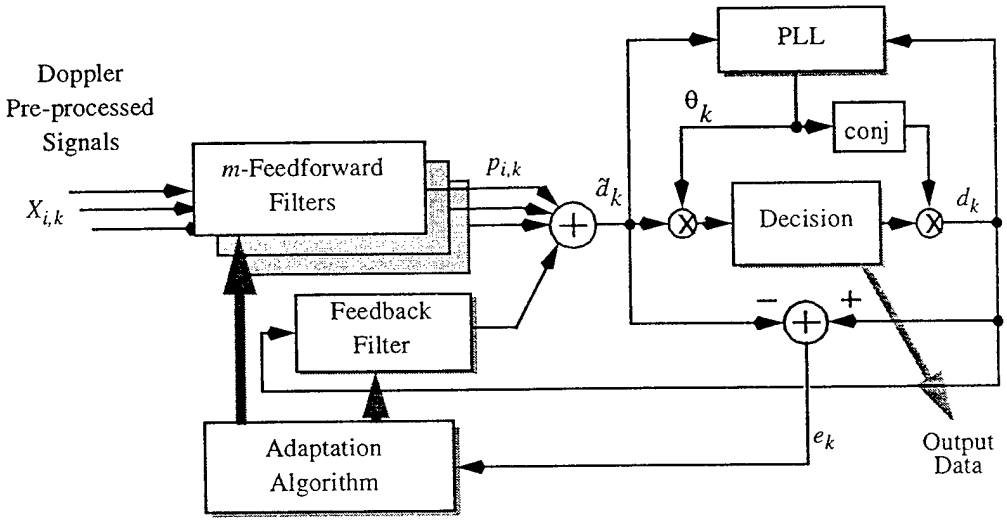

Fig. 7. The Decision Feedback Equalizer with multichannel input and single phase-locked loop.

There are three primary settings that govern equalizer performance, two of them, the PLL gain and the tracking rate for the adaptation algorithm are values that are used within the core of the equalizer. The third is the SNR threshold which each arriving multipath is compared with to determine whether or not it requires support in the feedforward and feedback sections of the equalizer. This "parameterization" is done as a pre-processing step before equalization.

The following sections focus on (1) the PLL and its performance with respect to gain, (2) the RLS update and selection of optimal tracking rate and, (3) the effect of different numbers of parameters upon the setting of the optimal tracking rate. Items (2) and (3) motivate the subsequent section: RLS and LMS algorithms with self-optimizing tracking rate.

PLL Gain

One of the more difficult values to determine for an unknown underwater channel has been the PLL gain. This is particularly true when both source and receiver are in motion and their relative velocities are changing over time. Performance can be varied from poor (many errors or even de-convergence of the equalizer) to excellent (no errors) simply by changing the filter loop gain. Often even a small change in gain will cause a disproportionate change in output mean-square error. Part of the problem is the interaction of the PLL with the RLS update algorithm: the RLS, when operated with the correct tracking parameter, is capable of providing phase correction when and if the PLL gain is too low to adequately estimate phase for a given data packet. However, the RLS equalizer cannot always provide good phase tracking. For example, when a large number of parameters are required and the tracking rate is slow, it will be unable to augment the PLL phase estimates to make up for shortcomings in the PLL. Conversely, when PLL gain and the track-

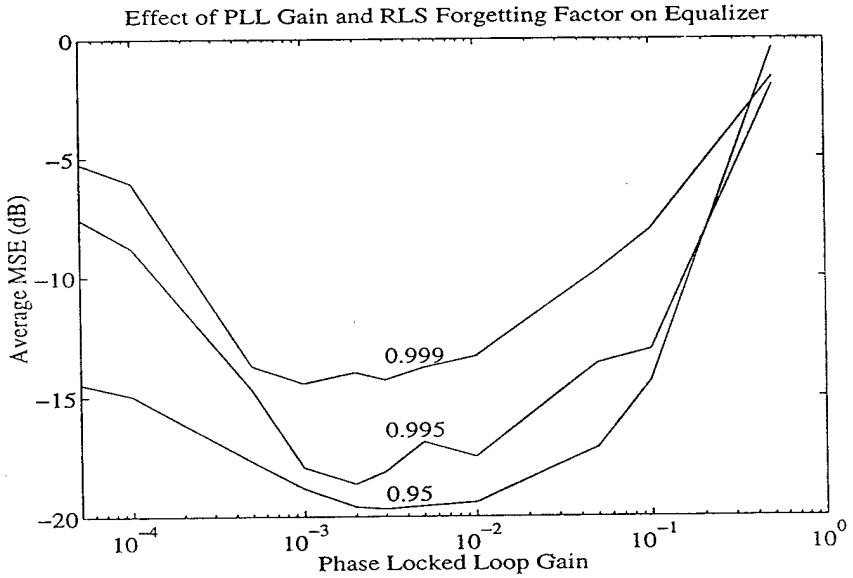

Fig. 8. Multi-channel PLL performance. The output metric is the average of the equalizer mean-square error (MSE) for the entire packet after training. The DFE is always operated with correct symbols fed back to compute the output error.

ing rate are both high, extraneous phase noise is introduced which lowers the total output SNR. The RLS (or other update algorithm) should not be depended upon to support inadequate phase tracking [5], and if the RLS *is* supporting phase estimates, modifying tracking rate can have unintended consequences on equalizer performance.

Any study of the performance of the PLL within the DFE is made difficult by this interaction between the RLS and the PLL. To study the PLL in a heuristic way, e.g. operating on real data, at a minimum the tracking rate of the RLS must be taken into account. Thus one must vary both the forgetting-factor as well as the PLL gain and examine the resulting two-dimensional performance space to determine the correct operating point. While earlier work [2] normally utilized a PLL for each input hydrophone, recent work by M. Johnson has shown that the single-PLL is more robust, particularly as the size of the feedforward filter increases. It offers equal or better performance than the multi-channel PLL of [2], at least for all of the vertical and towed array apertures currently under consideration. This would not be true when operating on multichannel data from a distributed array with the source, for example, in the center of the array.

Performance of the multi-channel PLL is shown in Fig. 8 and it is seen from this plot that the RLS forgetting-factor plays a large role in determining performance. When the forgetting-factor is 0.999 (long memory, slow tracking), the output MSE is governed primarily by the tracking rate and the bottom of the performance 'bowl' is flat. At the much higher tracking rate better performance is obtained but the range of gain values over which performance is uniform is narrower.

In Fig. 9 single-channel PLL performance on the same data packet is shown. Here the bottom of the performance 'bowl' is significantly flatter and it spans a much larger range than that of the multi-channel PLL. While the use of different RLS forgetting-fac-

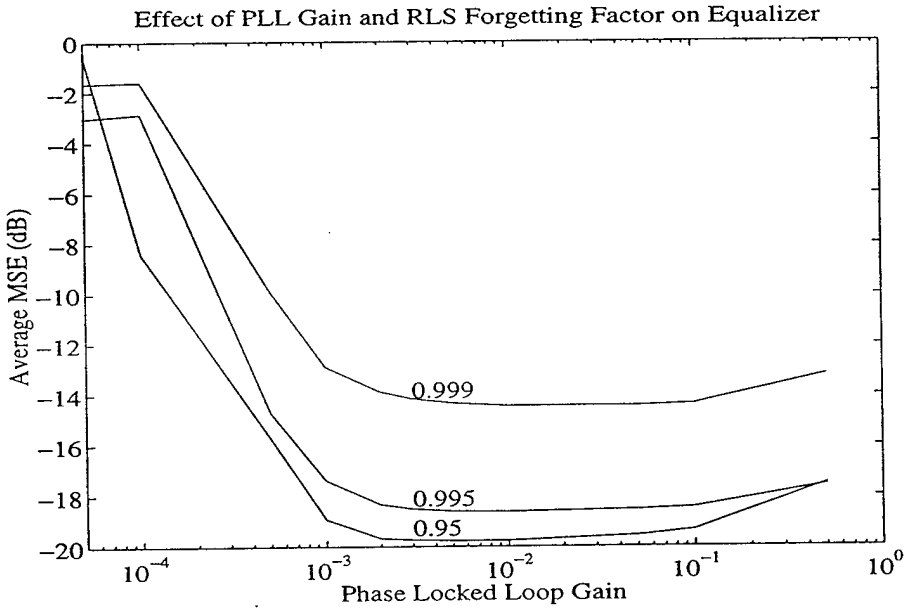

Fig. 9. Single-channel PLL performance. There is a broad range of near-equal performance across nearly two decades of PLL gain at all of the RLS forgetting factors.

tors certainly affects performance, the equalizer output is nearly constant over a very wide range of gain values. This demonstrates that, to a large degree, single-channel PLL operation is de-coupled from the RLS update portion of the algorithm.

With the performance of the PLL established and the selection of its gain greatly simplified, the next task is to examine the update algorithms and their control parameters in order to continue the process of reducing sensitivity to parameter selection and increasing performance on more complex channels.

Update Algorithms: RLS and Selection of the Optimal Tracking Rate

Two main families of update algorithms are normally used in acoustic communication: the recursive least-squares (RLS) and the least mean-square (LMS). When the RLS algorithm is used the forgetting factor λ must be determined before the equalizer is run, and similarly, LMS uses a tracking parameter, the step-size, to vary its tracking and convergence rate. A significant body of literature exists on these algorithms and their performance, however the objective of this discussion is to determine what is most appropriate for the underwater acoustic channel described in the introduction. In this section the direct form of the RLS algorithm is briefly reviewed, followed by examination of optimal forgetting factors for a range of underwater channels.

The RLS update to estimate the equalizer weight vector $\mathbf{h}_k$ given an input observation $\mathbf{x}_k$ and the desired output d_k requires the computation of the Kalman gain vector $\mathbf{k}_k$ and recursive estimation of the inverse auto-correlation matrix $\mathbf{R}_k^{-1}$. The direct form for an RLS update may be written as follows [6]:

Step 1, compute the new Kalman gain $\mathbf{k}_k$:

$$\mathbf{k}_k = \frac{\mathbf{R}_{k-1}^{-1}\ \mathbf{x}_k}{\lambda + \mathbf{x}^*_k \mathbf{R}_{k-1}^{-1} \mathbf{x}_k} \tag{1}$$

Step 2, perform recursive update of the weight vector $\mathbf{h}_k$

$$\mathbf{h}_k = \mathbf{h}_{k-1} + \mathbf{k}_k e^*_k \tag{2}$$

Step 3, perform recursive update of inverse auto-correlation matrix $\mathbf{R}_k^{-1}$

$$\mathbf{R}_k^{-1} = \frac{1}{\lambda}(\mathbf{R}_{k-1}^{-1} \quad - \mathbf{k}_k \mathbf{x}^*_k \mathbf{R}_{k-1}^{-1}\ ) \tag{3}$$

Step 4, compute the error using the equalizer output $y_k = \mathbf{h}_{k-1}\mathbf{x}_k$ and the known desired value d_k

$$e_k = d_k - y_k \tag{4}$$

It is well-known that selecting the proper RLS forgetting factor λ is important for maximizing performance [7]. While a low forgetting factor speeds convergence and increases tracking ability, it also introduces extraneous adaptation noise by minimizing the time over which the system state estimates are made. In a stationary environment setting the forgetting-factor to one (infinite memory) provides best ultimate performance, while in a time-varying environment the optimal value for the forgetting factor is highly dependent on the SNR, system order and its rate of change.

The best forgetting factor for the multichannel DFE combined with RLS parameter update operating on realistic ocean acoustic channels appears to vary between about 0.98 and 0.999. In terms of symbol memory this spans 50 to 1000 symbols, a significant range. Low forgetting factors are optimal for channels that are variable or that have high SNR and few parameters. The higher forgetting factors are appropriate for channels with any or all of these characteristics: relatively stable, low-SNR or heavily parameterized. Single-channel equalizers operate well at an even lower forgetting factor. In one, admittedly close-range and highly dynamic case, the optimal forgetting factor is found to be as low as 0.93 (14 symbols).

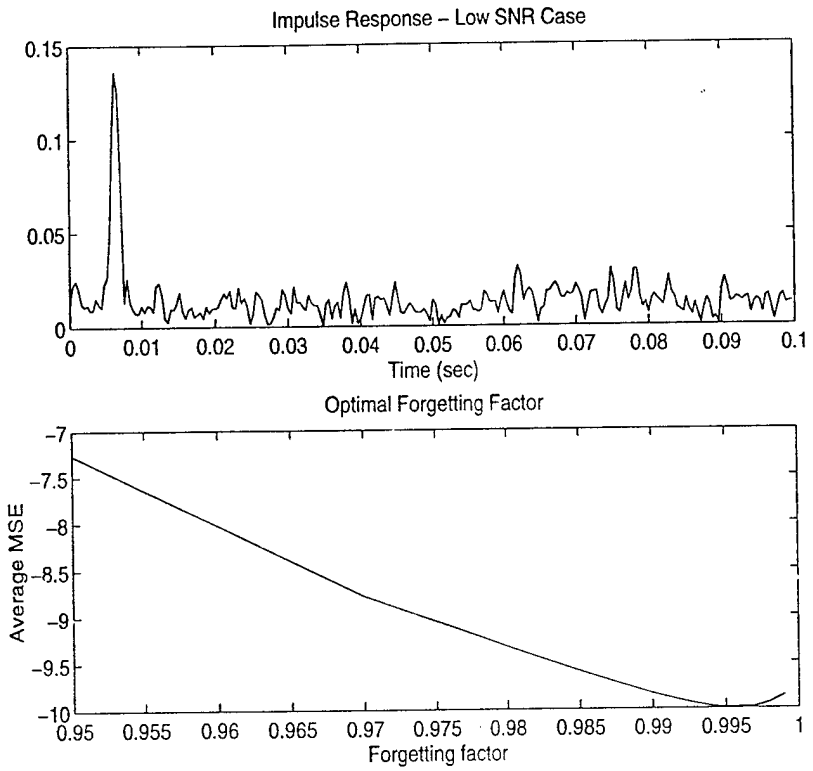

Fig. 10. Case 1. Simple channel with relatively low SNR. This channel was observed during tests offshore Ft. Lauderdale in about 50-200m water and a range of about 2 km. Bathymetry is variable and the sound speed profile was downward refracting.

Discussion of the underlying mechanisms which determine the optimal forgetting factor is made difficult because the number of hydrophones and the total number of parameters have such a large effect. While the issue of parameterization and its effect on proper selection of the forgetting factor will be discussed below, it is pointed out here that we are already at a disadvantage in pre-selecting the forgetting factor for a particular acoustic channel since knowledge of variability does not guarantee that the forgetting factor can be properly determined *a-priori*, nor does the total number of parameters selected for equalization, or the input SNR indicate explicitly how to choose the best forgetting factor.

Case 1: Low-SNR, Low-Complexity

Stable channels with low SNR utilize a forgetting factor close to 1 in order to optimize performance. This essentially provides averaging over a longer period of time and improves the estimates of the inverse auto-correlation matrix, for example. Only one arrival, with almost no spreading, is present in the example channel shown in Fig. 10. Some additional diffuse energy may be present between 0.06 sec and 0.09 sec, but the amplitude is low and adding feedback support over this area adds more noise than the system gains through equalization of this very low amplitude multipath. Using four hydrophones of

data with 6 feedforward taps per channel and 7 feedback taps, best performance is achieved at a forgetting factor of 0.995. Thus, the 200 symbol memory length provides the best compromise between tracking and residual mean-square error for this particular acoustic transmission channel.

Case 2: High-SNR, High-Complexity

For high-SNR situations with significant amounts of dense multipath the best setting for the equalizer forgetting factor is similar to that of the low-SNR, low-complexity case. This comes about because of the large number of parameters necessary to equalize a highly reverberant channel and because this channel, though complex, is changing relatively slowly over time. Four channels were used for processing, each with 12 feedforward parameters. Feedback support of 35 taps was provided for a total of 83 parameters. When configured in this fashion the optimal forgetting factor for the RLS equalizer is about 120 to 150 symbols, slightly less than Case One above. In should be noted however, that additional feedforward and feedback parameters, up to about 200 total, can be added to improve overall performance for this channel, and that the best forgetting factor continues to slowly increase as the number of parameters increases.

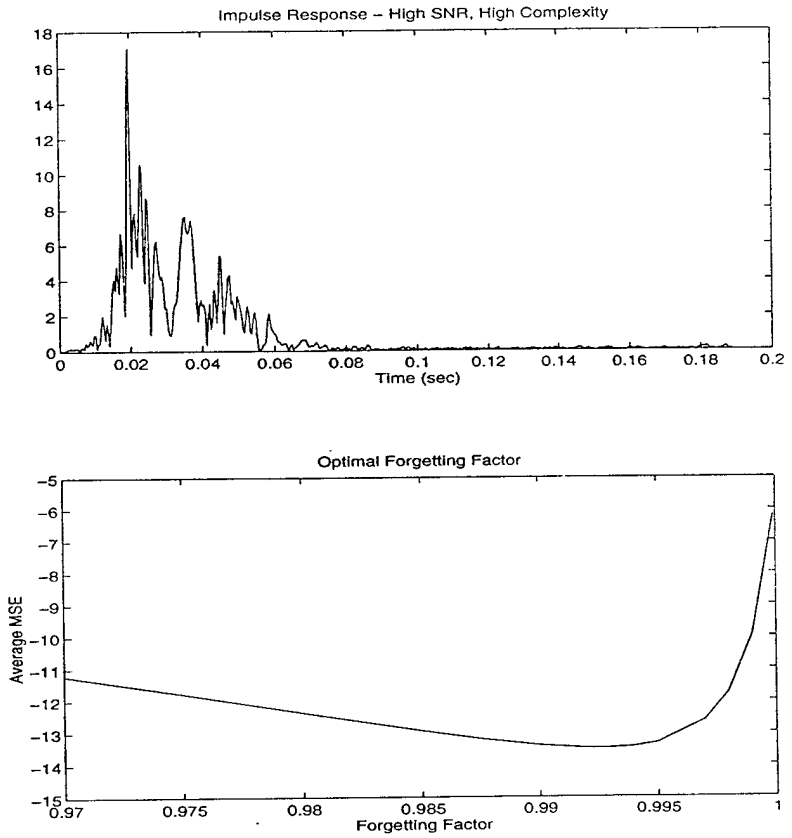

Fig. 11. Case 2. Impulse response and optimal setting for equalizer forgetting-factor for a shallow-water, moderately long-range channel (about 16 miles).

However, when the additional parameters are added the ability of the equalizer to track changes in the channel is eventually reduced and there is a complicated relationship between parameterization and selection of forgetting factor to achieve the best overall performance. Fortunately, despite the apparent complexity of this channel is it not difficult to achieve the MMSE necessary for error-free QPSK data transmission, however for higher-order constellations the additional 2-3 dB performance improvement available by increasing the feedforward and feedback filter sizes is important.

Case 3: Moderate SNR, Sparse Channel, High Complexity

While the channel described above has many closely-spaced arrivals, each with varying amounts of energy, other channels may have a lone initial arrival followed some time later by additional rays. This is the case in the channel shown in Fig. 12. The optimal parameterization for this channel is sparse and only a few feedforward taps are needed to span the first arrival, while feedback support is primarily needed from 0.06 to 0.08 s after the start point. The best possible performance is achieved at 50 parameters total, with optimal lambda of 0.988 or about 80 symbols but the output SNR achieved by the equalizer is still just below the level needed for low error-rate QPSK communication.

It is instructive to examine the effect of adding additional parameters in order to compare sparse feedback performance with that of a complete feedback section. Fig. 12

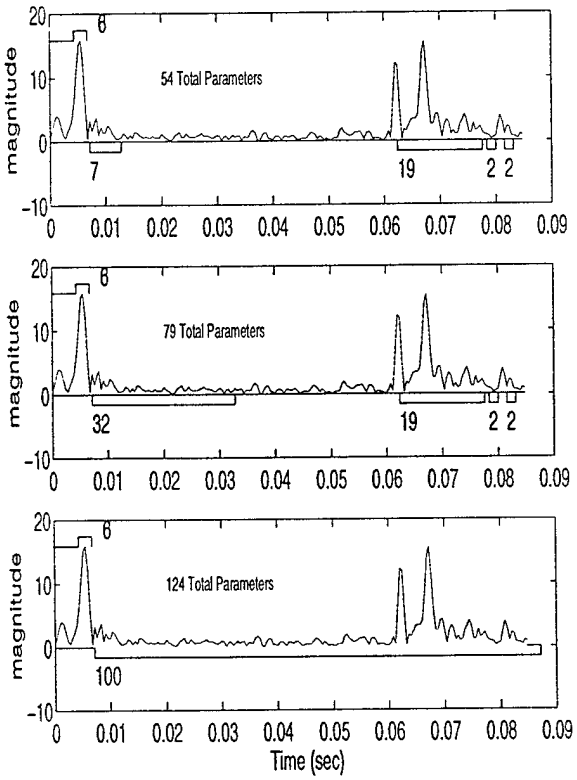

Fig. 12. Case 3. Impulse response and feedforward/feedback tap placement for three different runs to determine optimal forgetting factor in the presence of over-parameterization or with a non-sparse equalizer. In all cases 6 (T/2 spaced) feedforward parameters are used per channel. Feedback support is varied as shown by the lines drawn under the impulse responses and the numbers indicate how many taps are used in each section.

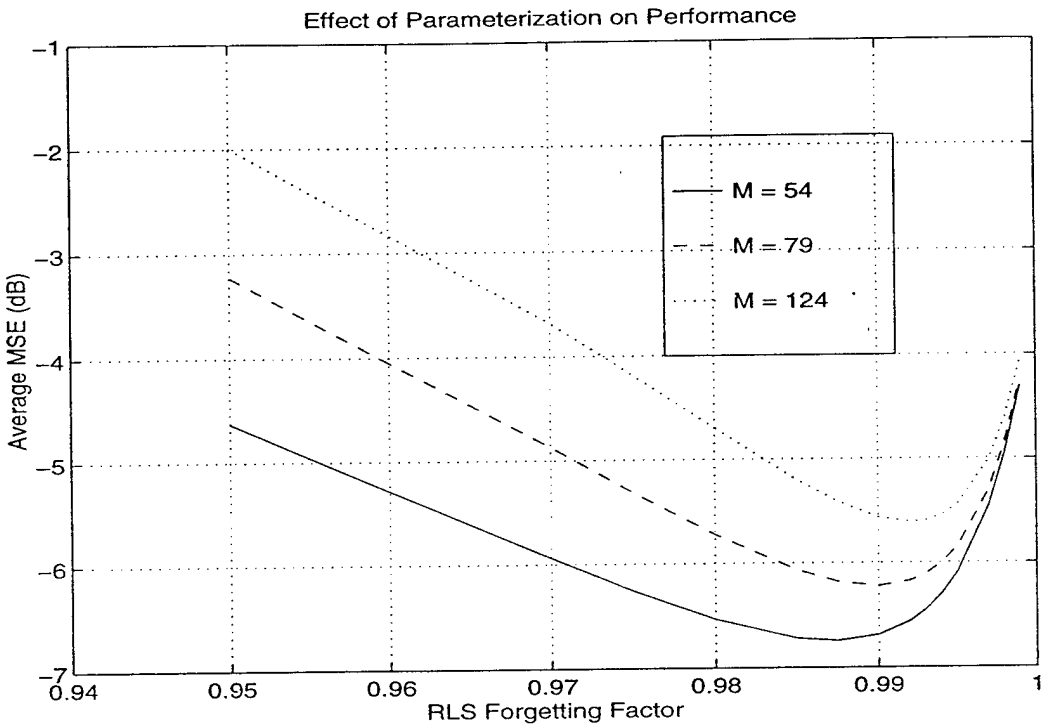

Fig. 13. Case 3 Parameterization Tests. The effect of adding additional parameters over the minimum optimal number (where M is the total of the feedforward and feedback) is to push the optimal setting for forgetting-factor higher and increase the mean-square error. This is due to the additional adaptation noise that is introduced. In this case the additional parameters are superfluous, as would be the case if a non-sparse equalizer was used on this sparse channel.

shows the impulse response and placement of feedforward and feedback taps for three different parameterizations. In all cases 6 feedforward taps are used on each of the four hydrophones. The topmost plot shows the minimum parameterization: only the absolute minimum number of feedback taps are used, and these provide support over the main arrival and the later group of incoming rays. In the middle plot 25 extra parameters are added arbitrarily after the main arrival and in the bottom plot full (non-sparse) parameterization is shown.

The results of equalizing with these parameterizations is shown in Fig. 13 where it may be seen that performance decreases as additional parameters are added, and that the best value for the forgetting-factor increases with additional parameters. Minimum (and correctly placed) filter taps allows faster tracking (and, of course, faster processing), while at the same time avoids adding noise from gratuitous equalizer parameters.

Case 4: Single Hydrophone Channel, High SNR, Modest Complexity

At high SNR or with modest complexity only a single hydrophone may be needed to successfully decode an acoustic packet, even if it is non-stationary. For example, the channel shown in Fig. 13 has only two primary arrivals, however we see the envelope of the signal fading over the course of the packet, indicating a degree of channel variability. The optimal forgetting factor for this channel depends, as always, on the total number of

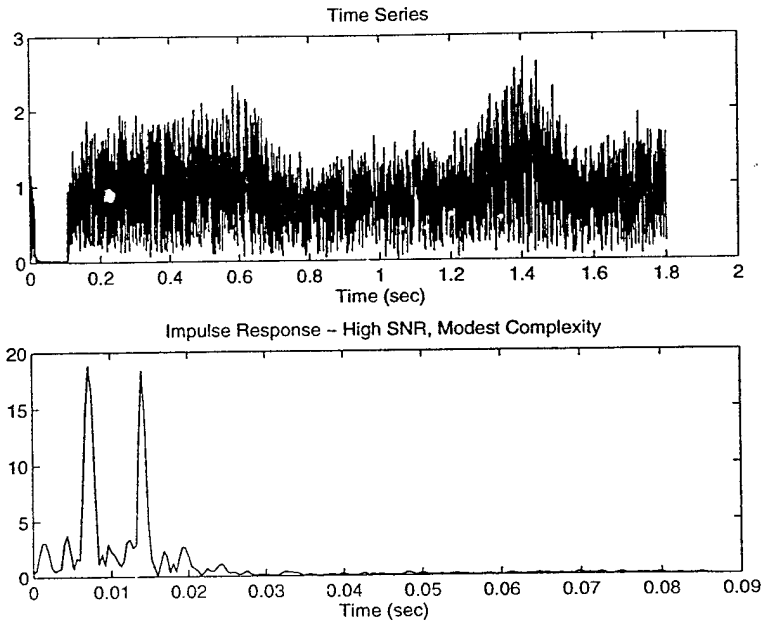

Figure 14. Case Study 4. High SNR data packet with two significant arrivals. This data is analyzed using a single hydrophone.

parameters used in the equalizer, but it is significantly lower than any of the multi-channel data examined earlier. When 12 feedback parameters are used (enough to provide equalizer support for the second arrival) optimal performance is achieved at 0.93, which corresponds to a memory of about 14 symbols.

This example points out the difficulty in selecting the proper forgetting-factor for the RLS: if one had followed previous cases and set the forgetting-factor to about 0.99 to 0.995, the equalizer output MSE would be greater than -5 dB, not low enough to operate the DFE and the packet would have not decoded at all. In contrast, with the correct forgetting factor and reasonably close parameterization, performance is quite good, -10 dB MSE.

As with Case Study 3 the performance of the algorithm with different numbers of feedback taps yields some sensitivity information about the forgetting-factor settings. When only 8 feedback parameters are used the second arrival has no support in the equalizer and performance is poor (the 'x' line in Fig. 15). As the number of feedback taps is increased to 12 and the second arrival is covered, performance is maximized (the 'o' line in Fig. 15) and is better by about 3 dB than the trial with only 8 taps. As additional parameters continue to be added (i.e. if the receiver is not intelligent enough to determine where the feedback taps need to be placed) performance deteriorates, slightly at first (the '*' line in Fig. 15) and then to a level ('+') even worse than the 8 parameter case.

The examples of Case Studies 3 and 4 point out not only the problems with selecting the RLS forgetting factor but as well illustrate the care that must be applied to parameterization. The following points can be made regarding parameterization and equalization:

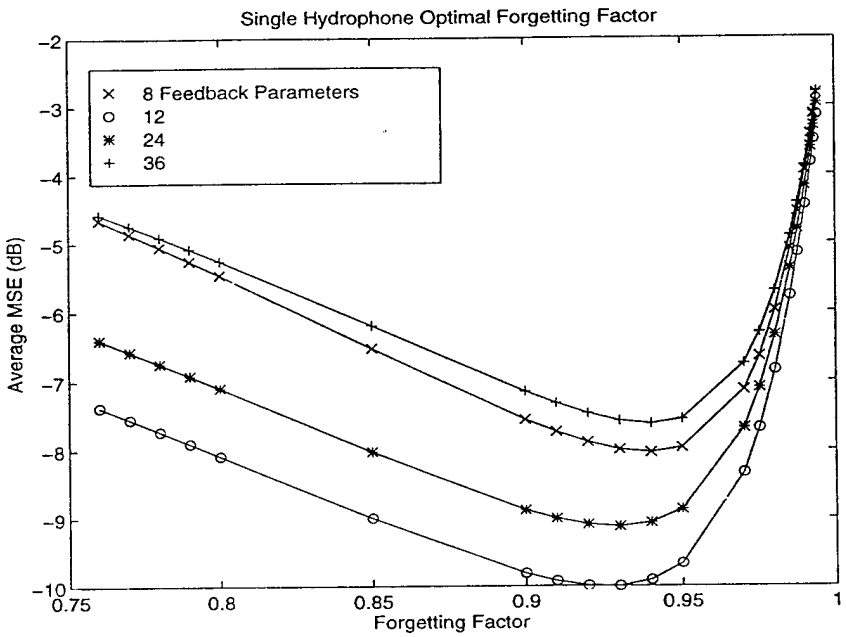

Fig. 15. Case Study 4. With the number of feedforward parameters held constant, the number of feedback parameters and the forgetting factor are varied to demonstrate the optimal operating point for the impulse response of Fig. 14. A total of 12 feedback parameters provides coverage for both significant arrivals and best performance is at a much lower forgetting factor than other channels described here. Eight parameters is insufficient to cover the 2nd arrival and performance is poor ('x'), while more than 12 parameters decreases performance ('*' and '+')

- A sparse equalizer (i.e. selective rather than complete feedback tap placement) is a requirement for sparse channels. In Case Study 3 the minimum parameterization shown offers best results and is still barely adequate for QPSK. Complete feedback coverage increases the mean-square error to a point where the DFE may diverge.
- Adaptive determination of feedforward tap width and feedback tap width and placement is required. Making guesses about maximum channel delay compromises performance by (1) adding superfluous taps when the delay spread is lower than expected, and (2) leaving multipath un-equalized when more multipath is present than expected.

Fortunately, a simple process has been developed for selecting thresholds to use in selecting filter tap locations. A description of this method will be left to a future work.

Adaptive-Memory RLS

As demonstrated by the above examples, for the RLS to provide optimal performance the correct forgetting factor must be used. While a set of heuristic rules can be established based on the total number channels and parameters, this cannot be optimal because it does not take into account the degree of variability of the acoustic channel. Thus a method which can set or adapt the forgetting factor as required by the channel is needed.

The use of the adaptive-memory RLS (adaptive-memory means modifying the forgetting factor over time) allows optimal tracking over the period of a single packet or over many packets, depending on the learning rate of the algorithm. The learning rate controls the update of the forgetting factor and the overall time scale of the adaptation. Thus the adaptation rate for the entire system can be chosen to be very fast (e.g. for a UUV that is continually moving through different acoustic channels), or quite slow (e.g. for a geographically fixed system where the acoustic channel changes over tidal time scales).

The adaptive-memory RLS is derived from a cost function which minimizes overall estimation error based on optimization with respect to λ [7][11]. The standard RLS algorithm is augmented with three additional equations, one, the derivative of the inverse autocorrelation matrix estimate, two, the matrix gradient, and three, the current estimate of the forgetting factor. All of the equations are recursive updates.

The estimate for the derivative of the inverse autocorrelation matrix is given by:

$$\mathbf{S}_k = \frac{1}{\lambda_k}(\mathbf{I} - \mathbf{k}_k \mathbf{x}^*_k)\,\mathbf{S}_{k-1}\,(\mathbf{I} - \mathbf{x}_k \mathbf{k}_k^*) + \frac{1}{\lambda_k}(\mathbf{k}_k \mathbf{k}_k^* - \mathbf{R}_k^{-1}) \tag{5}$$

while the gradient is

$$\psi_k = (\mathbf{I} - \mathbf{k}_k \mathbf{x}^*_k)\,\psi_{k-1} + \mathbf{S}_k \mathbf{x}_k e_k \tag{6}$$

and the forgetting factor is

$$\lambda_k = \lambda_{k-1} + \alpha \mathrm{Re}\,(\psi^*_{k-1} \mathbf{x}_k e^*_k) \tag{7}$$

where α is the learning coefficient and 1_k is limited at each time step between a range $\lambda_{min} < \lambda_k < \lambda_{max}$ whose limits are set in advance.

While this algorithm works quite well, there several issues which affect its use in a practical system at this point in time:

- The equations are based on the *n*-squared RLS algorithm which is sensitive to round-off error when performed in single-precision arithmetic. On most 32-bit DSP-based systems the square-root RLS is used because of its superior numerical stability. The adaptation equations are not directly transferable to the square-root algorithm because different quantities are being calculated (e.g. the *square-root* of the estimate of the inverse autocorrelation matrix). Thus the equations above would have to be re-derived in the context of the square-root algorithm and their sensitivity to single-precision arithmetic established.
- The computational complexity of the equations is quite high. The RLS is already $O(n^2)$, and the load imposed by, in particular, the derivative of the inverse autocorrelation matrix (eq. 5 above) makes this algorithm several times slower than the standard RLS.

Examples

In order to demonstrate that the adaptive memory RLS does indeed converge to the optimal forgetting factor, a set of equalizer runs at different forgetting factors was performed in order to determine the best value, and this was then compared with the output of the adaptive algorithm described in the equations above. In Fig. 16, the top plot shows the optimal forgetting factor curve which indicates that 0.985 provides best performance. In the lower plot of Fig. 16 it is seen that the adaptive algorithm converges to 0.985 after 1800 symbols. Convergence can be made faster at the cost of additional sensitivity in the estimate of the forgetting-factor, or slowed to smooth out small-scale changes in the channel variability.

To demonstrate convergence from a wide variety of starting points (important because the system must still be provided with an initial value), the adaptive algorithm was run with different initial guesses. In Fig. 17 convergence to the same final value for any starting point is shown. This result is as expected and allows some freedom in selecting the starting point without the concern that it would be outside a critical range. As in Fig. 16, the learning rate is such that the forgetting factor has converged after about 1800 symbols.

In a high data rate system there would be no reason to continually restart each packet with the same pre-set value. Instead the final output of the preceding packet would be used at the start of the current packet. If this is done then the learning rate can be lowered and the system will slowly adapt the forgetting factor over a few packets, which at high symbol rates (2000-5000 sps) may only be a few seconds depending on packet length.

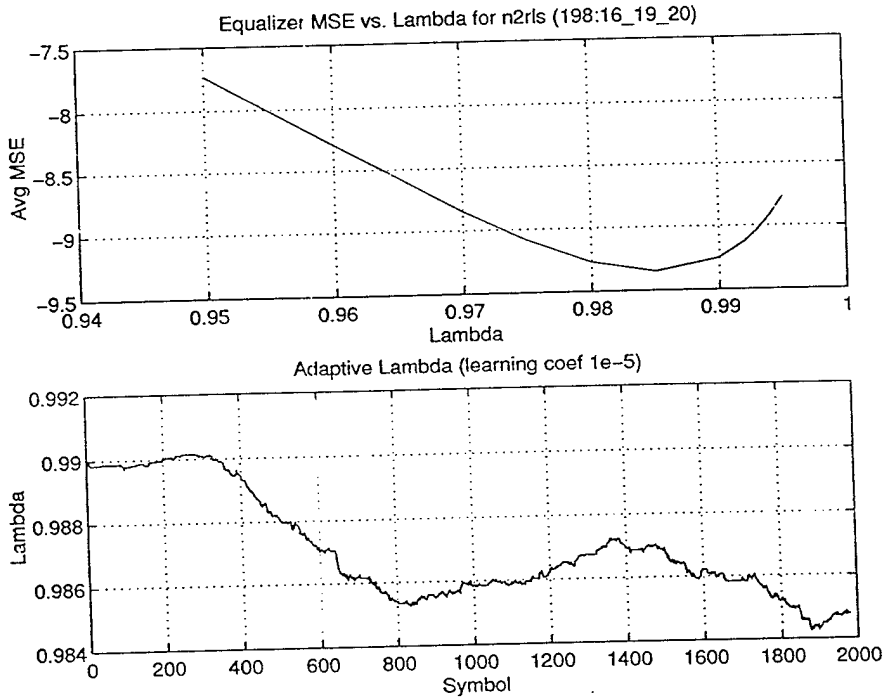

Fig. 16. Optimal forgetting factor determined through multiple equalizer runs (top), and convergence of the adaptive algorithm to the best value after about 1800 symbols.

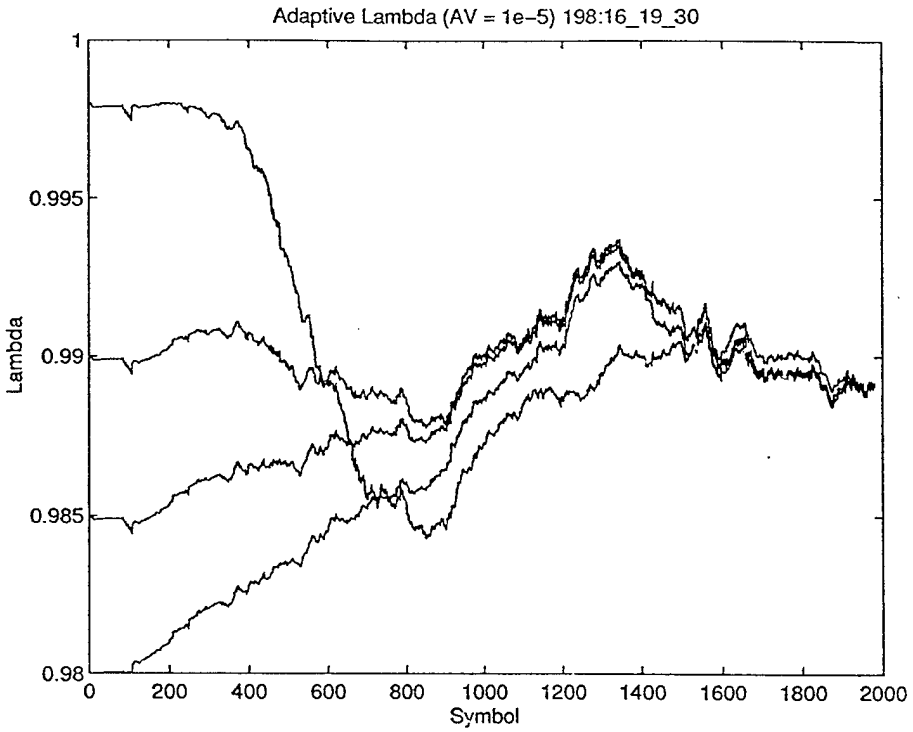

Fig. 17. Evolution of the optimal forgetting factor from a number of different starting points. Concerns about proper initial values are eased because of the convergence properties of the algorithm.

Sensitivity of the equalizer to the learning rate value is relatively low. While the forgetting factor evolution over time may appear noisy when the learning rate is high, since it is a 2nd order control parameter the overall MSE of the equalizer does not change drastically when the learning rate is changed. This can be demonstrated by comparing the adaptively-computed forgetting factor at different learning rates with the actual performance change of the equalizer. In Fig. 18, low, medium and fast learning rates are used on different runs of the equalizer and there appears to be a large difference in the resulting forgetting factors. However, when the equalizer output MSE for a range of learning rates is plotted (Fig. 19), it is seen that there is only 0.02 dB difference between the slow and medium tracking settings, and virtually no difference between the medium and fast.

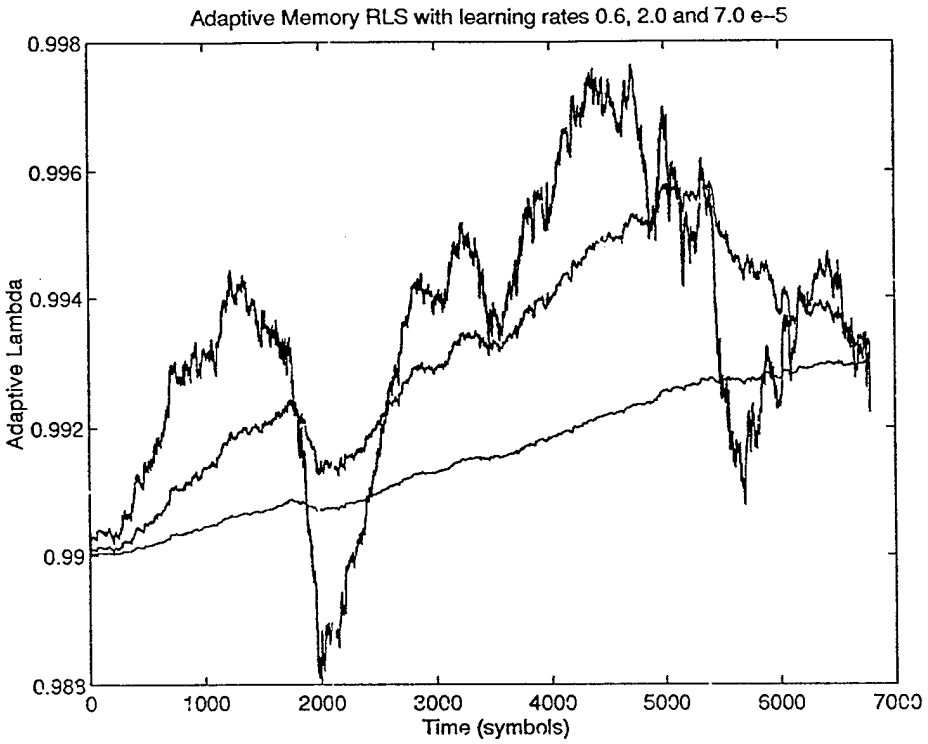

Fig. 18. Evolution of forgetting factor with different learning rates.

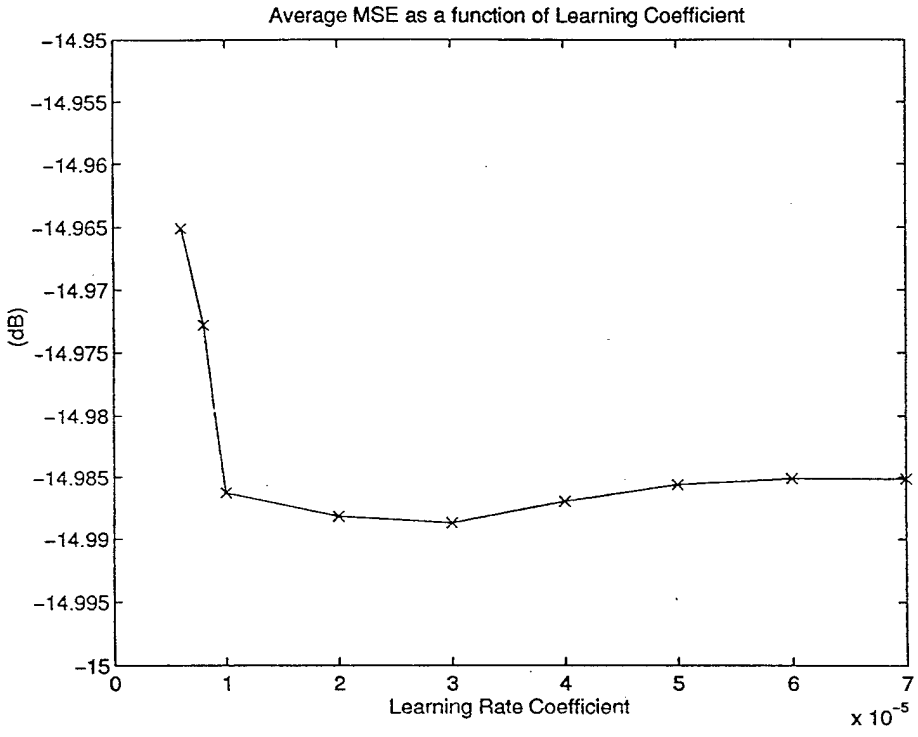

Fig. 19. Equalizer MSE output for different learning rates. Only a very small difference in output performance is present despite the large change in learning rate and the apparent noise of the estimate shown in Fig. 18 above.

Adaptive Step-Size LMS

The LMS algorithm with adaptive step-size requires computing the time-varying step-size μ_k and the gradient estimate Y_k. These are given by [11]:

$$Y_{k+1} = (I - \mu_k \Phi_k \Phi_k^H) Y_k + \Phi_k e^*_k \text{ and} \tag{8}$$

$$\mu_{k+1} = \mu_k + \alpha Re(Y_k^H \Phi_k e_k) \tag{9}$$

where α is a small learning-rate variable, I is the identity matrix and Φ_k is the regressor vector at time k. The outer product in (8) is order-n^2 in computation so it is re-written as

$$Y_{k+1} = Y_k - \mu_k \Phi_k (\Phi_k^H Y_k) + \Phi_k e^*_k . \tag{10}$$

The standard LMS equations are much more computationally efficient than the RLS equations (order-n rather than n^2), so the addition of the adaptive step-size update equations (9) and (10) is almost immaterial as long as the performance of this algorithm is close to that of RLS.

There is a wealth of literature on the LMS algorithm and a number of publications about the adaptive step-size version [1][4][7][8][11]. The adaptive step-size LMS has been used for underwater acoustic communication before [9] [10][11], but not with the same equalizer structure presented here. In addition, detailed comparisons over large data sets have not been published. Here we focus on actual use of the algorithm and comparison with RLS for the multichannel DFE with 2nd order PLL as described above.

Fig. 20 shows the performance comparison of the two algorithms for a set of about 180 data packets which have a range of different SNRs and multipath complexities. In general the RLS performs just fractionally better, normally 0-1 dB. In several cases the LMS is slightly better (about 1 dB). This data set is a challenging one and 23% of the

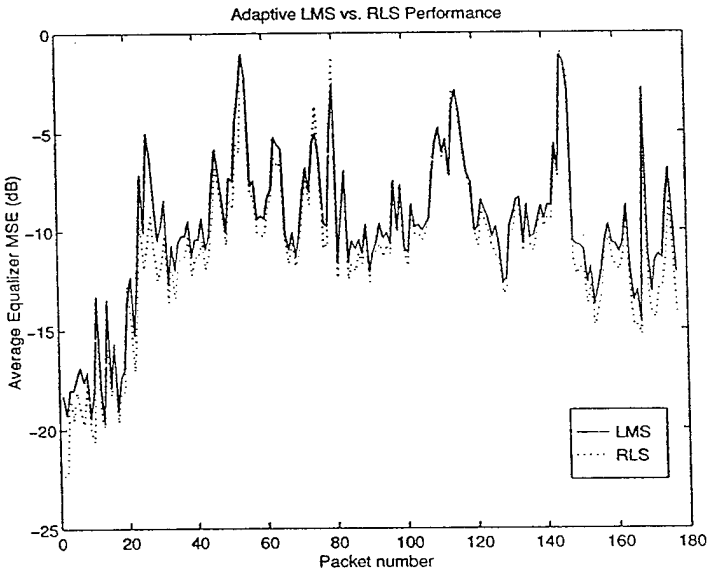

Fig. 20. RLS vs. LMS performance over 180 packets collected during a moving-source/receiver test offshore Ft. Lauderdale. The acoustic channel varies from high to low SNR and low to high complexity.

packets have errors when processed with RLS. When repeated with LMS, 28% of the packets have one or more errors. This relatively small difference is reasonable, many of the packets have almost identical performance but there are a number of packets which have higher complexity and dynamics that will be more appropriate for RLS.

That this example demonstrates that often the RLS and adaptive step-size LMS perform equivalently, and that there are a number of circumstances where RLS is superior, is not surprising based on a study of the adaptive filter literature (for example, [13]). However, in the acoustic communications literature there has been some polarization about the use of the two algorithms with a number of researchers declaring that LMS was superior and others taking the view that it was completely unsatisfactory. This is most likely due to the different equalizer structures or update algorithm implementations that were used by the different investigators. For example, some did not jointly optimize over all parameters, but instead operated over channels individually [10]. In addition, before the publication of [5], Doppler pre-processing to compensate for time dilation had not performed in conjunction with equalization. One of the reasons often cited for not using LMS is its convergence time, however as will be shown below, there are several approaches to overcoming this, none of which has appeared in the literature at this time.

An added complication to the debate is that most investigators have been using different data sets taken under different conditions. It is quite logical that those with LMS compatible data would use that algorithm, while those with more complex data requiring faster tracking and convergence would use RLS. A direct comparison across three different types of acoustic channels using both single and multi-hydrophone realizations in presented in Appendix B.

To demonstrate that the adaptive step-size LMS algorithm is operates as expected, it is useful to examine the algorithm-derived step-size with respect to both the channel SNR at the input and the number of parameters used (which is estimated adaptively and is

a measure of channel complexity). Fig. 21 shows that, indeed, high SNRs support larger step-sizes while the low SNR data often requires a smaller step-size to adequately estimate equalizer parameters. The relatively large range of step-sizes at a given SNR is due to differences in dynamics and differing numbers of parameters.

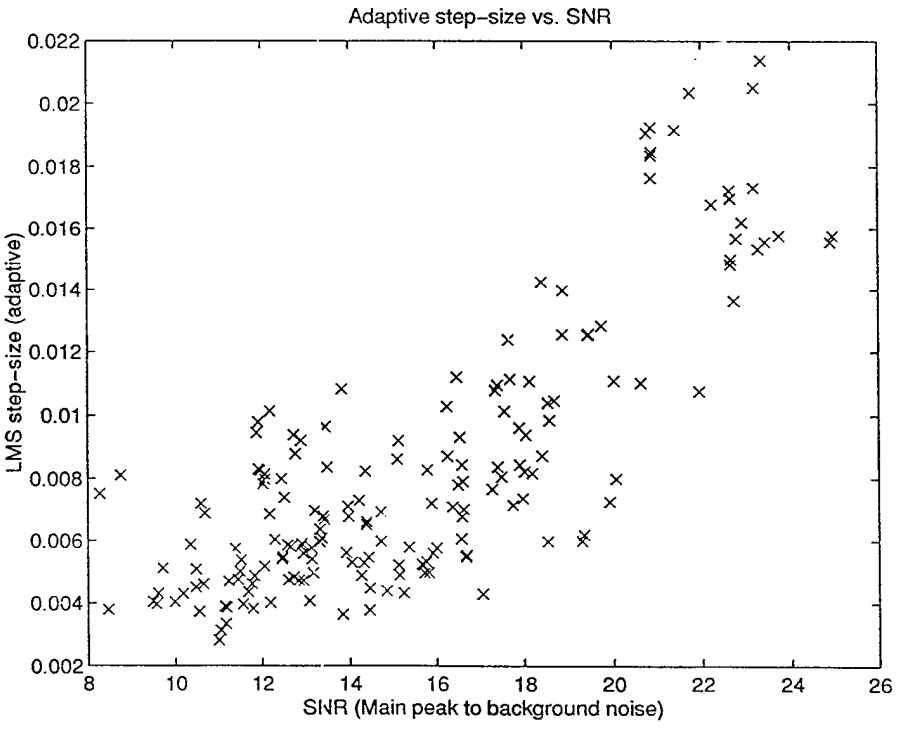

Fig. 21. Step-size from the adaptive LMS plotted vs. SNR for the 180 packets shown in Fig. 20.

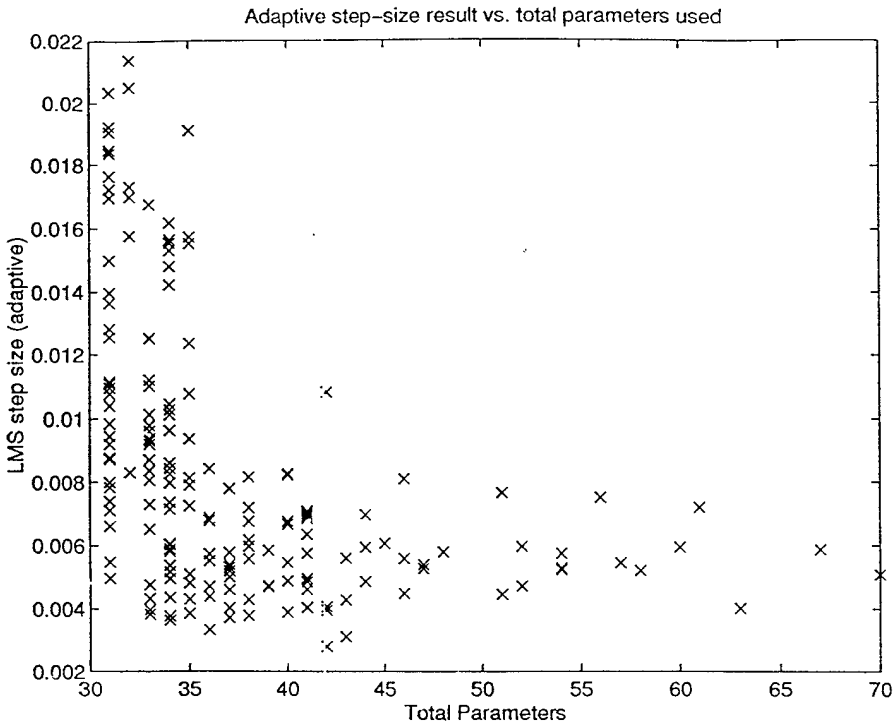

Fig. 22. Step-size from the adaptive LMS plotted vs. number of parameters (which is automatically determined from the impulse response of each packet) for the 180 packets shown in Fig. 20.

In Fig. 22 the adaptively determined step-size for different numbers of equalizer parameters is shown. As expected, when larger number of parameters are used the step-size is low, while when less than about 40 parameters are used the step-size can range over a wide set of values, as dictated by tracking considerations.

Convergence

One of the main problems with using the LMS algorithm is its slow convergence. The fractionally-spaced sampling of the equalizer, coupled with its multichannel structure means that the autocorrelation matrix has a banded form and potentially a very large condition number. Depending on the eigenvalue spread of the correlation matrix, convergence may be quite slow and require a large number of training symbols. While the RLS algorithm is insensitive to eigenvalue spread, it has a direct impact on LMS convergence. RLS normally converges in about 2*M symbols where M is the total number of parameters. LMS typically takes several times this which would require changing the packet structure from about 500 training symbols (out of about 7000 total) to several times that many. The resulting decrease in throughput is not acceptable and a method of speeding training is desired.

Two effective methods have been developed for coping with the slow convergence. One, detailed in Appendix B, is to use the RLS algorithm during training, then provide the final set of equalizer parameters to the LMS update algorithm after convergence. The LMS is then used for the remainder of the packet. While this works quite well, as the number of parameters increases to several hundred, the time that this takes (since RLS is so computationally intensive) begins to become too high and the advantage of LMS is lost.

Thus, as an alternative, a simple multi-pass approach has been developed which works as follows. At the end of training the output mean-square error is checked against that required for operation of the DFE without training data. If the equalizer has converged

and the MSE is low enough (about -8 dB for QPSK), then the algorithm can simply continue. However, if the MSE is not low enough for the DFE to provide error-free decisions then training is restarted using the last set of filter parameters, the gradient estimate and the most recent phase estimate. This method of 'bootstrapping' the LMS works very well, and it was found experimentally that using the last phase estimate from the PLL is important since the phase of the filter parameters and the PLL phase represent the aggregate phase of the equalizer.

The MSE performance of the multi-pass method is shown in Fig. 23. Without bootstrapping the equalizer converges in about 2000 symbols, four times the amount of training data available. The proposed approach has converged iteratively to a very low MSE which it then is able to maintain after training is completed.

An example of how the algorithm converges as training is repeated is shown in Fig. 24. For this particular data set convergence is exponential and there would be no point in continuing after about 8 passes. For QPSK signaling only one pass would be required, but for higher order constellations, for example 16 QAM, starting with -24 dB MSE would be a large advantage and well below the MSE level required for error-free DFE operation.

This method has been used on 8 channel data sets with over 1000 parameters total and it normally operates extremely well. The primary condition for convergence is that by the end of the first pass some progress, however small, must have been made towards proper estimation of the equalizer parameters. In practice this means that the MSE needs to be about 0 dB by the end of training, otherwise the 2nd pass is starting with no advantage and it is unlikely that the algorithm will ever converge. Fortunately, this condition is simple to detect and, if after several passes, no progress has been made, the approach can be abandoned in favor of a more complex solution such as RLS.

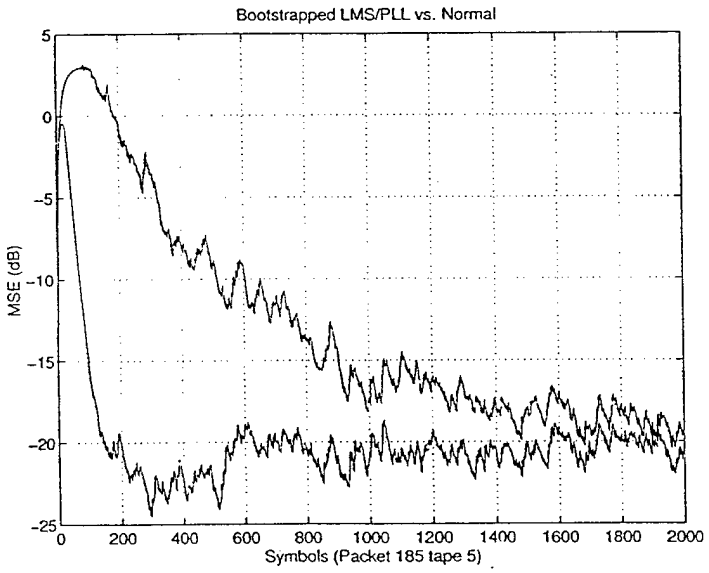

Fig. 23. Demonstration of the effective convergence of the multipass LMS compared to normal. The first 500 symbols were used repeatedly for training in the bootstrapped case and the full 2000 where used for the other.

Experimental Results

In this section some examples of equalizer operation are presented in order to demonstrate its effectiveness on both straightforward and difficult acoustic channels. First however, the beamforming capability of the equalizer is briefly presented.

In Fig. 6, during the discussion of different acoustic channels, the angles of arrival for a sparse impulse response at close range are shown. The first set of arrivals has angular spread of about 4 degrees, while later arrivals are separated from this main group by 7 to 15 degrees. During equalization it is assumed that the feedforward filters will exploit angular separation to reduce ISI, and that the feedback section will then remove the residual interference. To examine the effectiveness of the feedforward filters the output is correlated with the known data sequence to estimate the impulse response after this initial stage of processing. In Fig. 25 the channel impulse response for one hydrophone is shown, and below it the feedforward filter bank output. Of the 3 arrivals in the first group (this area had feedforward filter support), the combination of filtering and angular discrimination has sharpened the first peak and removed much of the following two peaks. Both the 2nd and 3rd arrivals are quite close in angle to the main arrival so their removal is presumed to be primarily through feedforward filtering and only partially due to beamforming. Of the second pair of arrivals the first ray is not removed completely since it is close (about 6 degrees) in angle to the main arrival, but the 2nd ray of the pair, which is separated by more than 15 degrees from the main group of three, is suppressed. Multipaths after this pair are completely suppressed as well, their separation from the main arrival is about 9 degrees. The output impulse response spans 20 symbol intervals whereas before feedforward filtering the total span was about 80 symbol intervals.

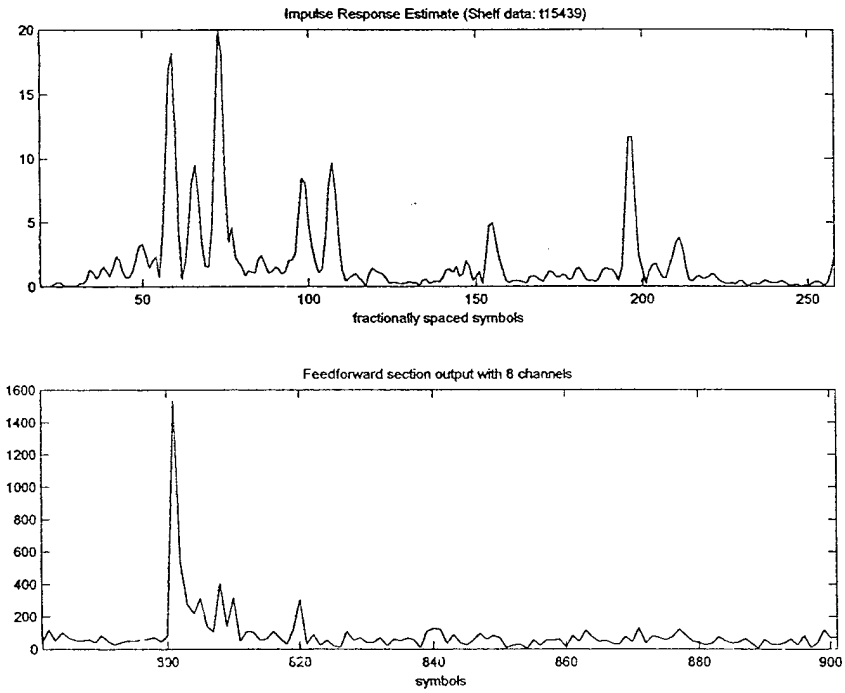

Fig. 25. Impulse response before and after feedforward filtering. A large amount of channel ISI is removed after this step, despite the fact that feedforward tap coverage is limited to the first group of three arrivals. The arrival angles for this impulse response are shown in Fig. 6.

As the multipath becomes more spread in time delay and less spread in angle, more feedforward taps are needed and the equalizer operates less as a beamformer and more as a linear combiner. However, as long as the number of feedforward and feedback taps are correctly chosen, this change in operation, from beamformer to optimal combiner, is automatic. The coherence length is also a factor in equalizer operation and thus arrays with closely space sensors are more likely to be implicitly beamformed than those with sensors spaced longer than the coherence distance of a particular channel.

The results shown in Figs. 26, 27 and 28 correspond to the channels shown in Figs. 1, 3 and 4 from the introduction. The first example, Fig. 26, is relatively close range (3.5 miles) and it is decoded without difficulty using adaptive step-size LMS with multipass training. However, some phase motion, a one Hertz sinusoidal signal, is also present. The PLL tracks this phase, which is superimposed on a linear trend, and the effect of whatever is causing the phase change is also seen in the equalizer mean square error. This phenomenon is most likely due to motion of the tow body on which the source is mounted, and is an example of an (unanticipated) non-stationarity which contributes to the overall dynamics of the channel. When the RLS is used on this channel the performance results are quite similar.

In Fig. 27 results are shown from data collected at 24 miles. Despite the significant increase in multipath complexity (three times as many feedforward taps are needed to span the impulse response), the output SNR is only somewhat lower than the 3.5 mile case. Since the source is motionless and Doppler is almost zero, there are no phase anomalies in this data packet. The comparison of the close-range results with the long-range results serves to illustrate that while distance contributes to multipath complexity in this environment, when input SNR is high an effective and properly parameterized equalizer is still able to achieve high output SNR regardless of range.

In Fig. 28 the results of equalizing the 11 mile 'wedge' channel (deep to shallow propagation) are shown. While at first glance this acoustic channel appears almost impossible to equalize the receiver structure presented here successfully decodes the packet. The SNR is lower than the preceding examples and there is a significant amount of long-delay, low-amplitude multipath. The Doppler shift is nearly the same as the first example, about 2.5 knots. The equalizer faces a serious challenge in this case, almost 1000 parameters are needed provide long feedforward filters for each channel, and an additional 100 parameters are used for feedback filtering. As with the first two examples, the adaptive step-size LMS with repeated passes through training is used. During the first 2 seconds after training the mean-square error is stable, but the MSE increases over time and ultimately several errors occur. There are 10 symbol errors that occur as the channel degrades, but they are corrected with a short block code during post-processing.

While the system is operating near its performance limit, many (but not all) packets similar to that of Fig. 28 can be decoded with few or no errors. Doubling the number of channels continues to improve performance (for example, the results shown in Fig 5 of Appendix B employ up to 15 channels).

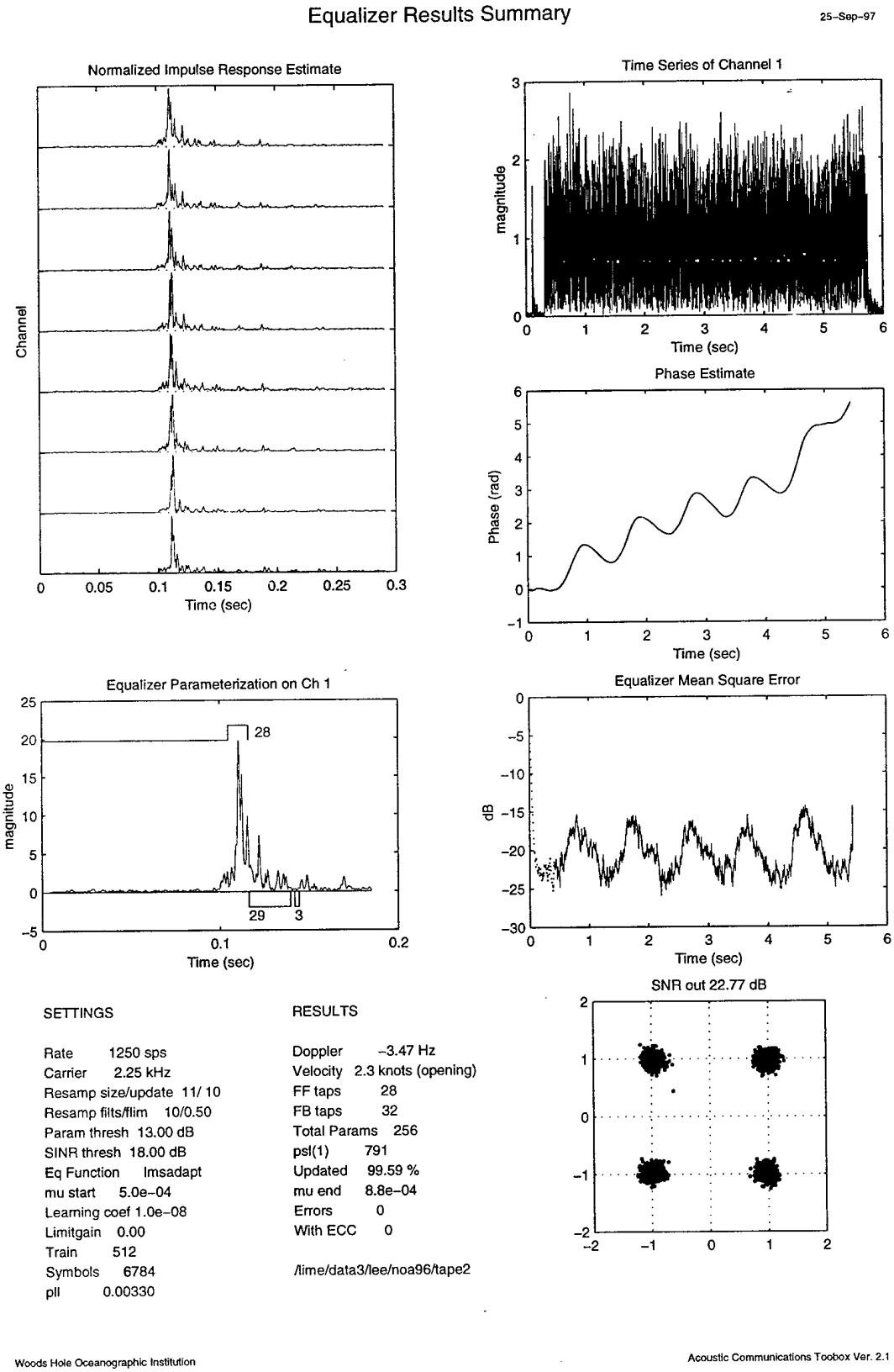

Fig. 26. 3.5 mile equalization results.

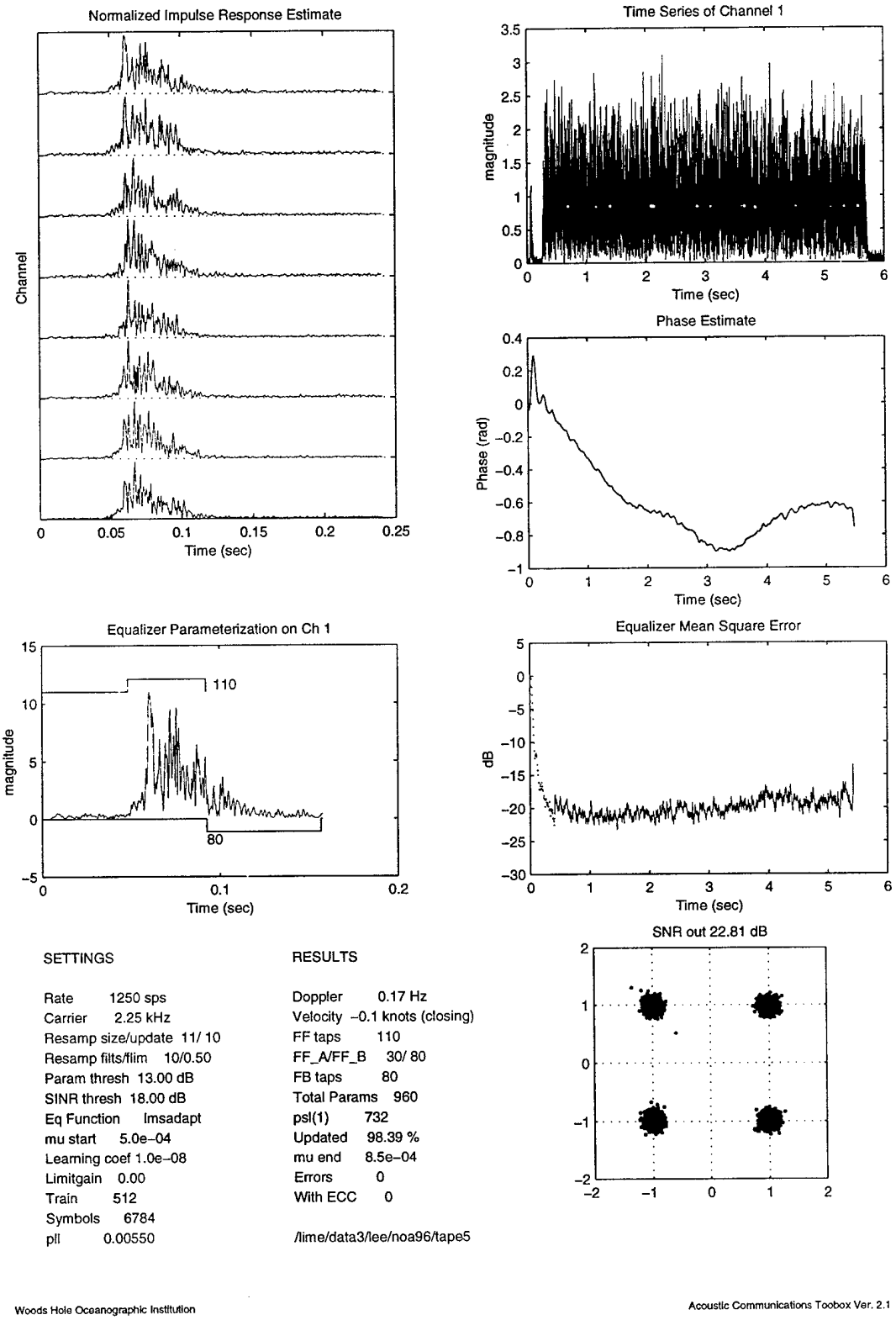

Fig. 27. 24 mile equalization results.

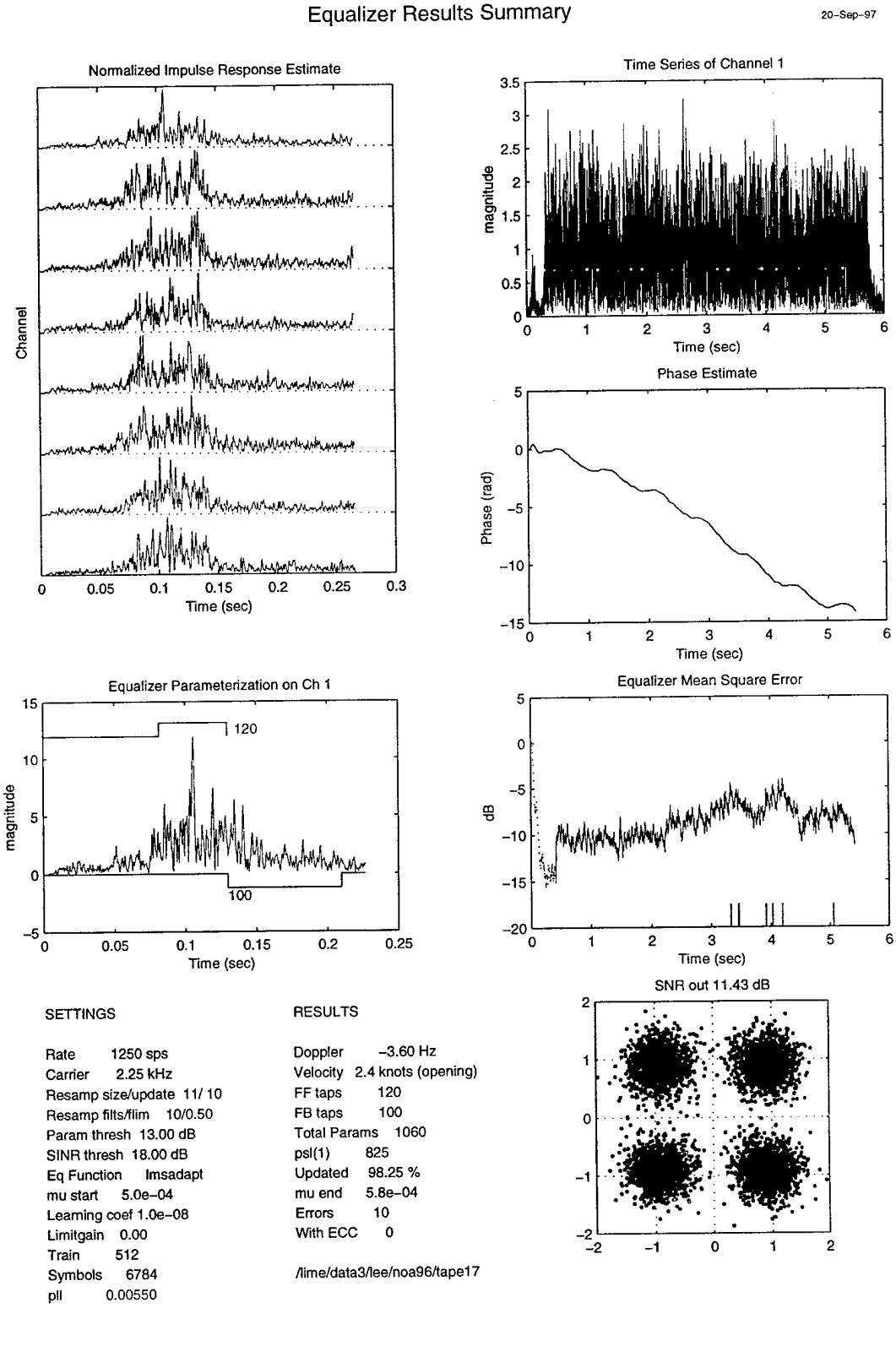

Fig. 28. 11 mile 'wedge' propagation equalization results.

Observations and Conclusion

While the results shown above demonstrate significant progress in coherent equalization, it is important to determine if much additional improvement might indeed be possible.

In Fig. 28, a difference of 3-4 dB is noted between the area where repeated training was done and where the equalizer resumes single-pass, decision-directed operation. If no change in MSE had occurred during this transition (as for example, in Fig. 23), then it could be concluded that, one, the channel is essentially stationary, or two, the equalizer is able to track channel changes perfectly. However, this is not the case and in addition, RLS provides no better performance, presumably due to the large number of parameters. Thus the following tentative statements can be made:

- The channel is stationary enough over 500 symbols (0.4 seconds) so that repeated application of the 1000 parameter LMS adaptive filter can reduce the MSE to a fairly low value (-14 dB).
- However, channel variability over longer periods is such that with this many parameters, in tracking mode the best performance possible with the LMS algorithm is about 3-4 dB worse than the best achieved during iterative training. The RLS algorithm provides very similar MSE results, presumably limited by adaptation noise that removes any tracking advantage that it might have had over LMS.
- Thus, the channel variability, coupled with the large number of parameters is limiting total performance and both LMS and RLS recursive algorithms are unable to achieve the optimal solution.

In one sense this is a satisfying conclusion because it leaves room for additional work on equalizers which attack this long multipath spread with a different approach. It also indicates that the complexity of the shallow-water channel in combination with this particular architecture is what limits the ultimate range possible. This extremely difficult channel, at even longer ranges, can still be considered usable for coherent communication though our approach to receiver design must continue to be examined.

References

[1] M. Stojanovic, J. Catipovic and J. Proakis, "Phase coherent digital communications for underwater acoustic channels", *IEEE J. Oceanic Eng.*, Vol. OE-16, pp 100-111, Jan. 1994.

[2] M. Stojanovic, J. Catipovic and J. Proakis, "Adaptive multichannel combining and equalization for underwater acoustic communications," *J. Acoust. Soc. Am.*, Vol. 94, No. 3, Pt.1, Sept. 1993.

[3] B. Widrow et al. "Stationary and non-stationary learning characteristics of the LMS adaptive filter", *Proc. IEEE*, Vol. 64, No. 8, August 1976, pp.1151-1162.

[4] M. Johnson, L. Freitag and M. Stojanovic, "Improved Doppler Tracking and Correction for Underwater Acoustic Communication," in Proc. *ICASSP '97*, vol 1, pp.575-578, Munich, Germany, April, 1997.

[5] L. Freitag, M. Johnson and M. Stojanovic, "Efficient equalizer update algorithms for acoustic communication channels of varying complexity," Proc. *Oceans '97*. Halifax, Canada. Oct. 1997.

[6] M. Johnson, D. Brady and M. Grund, "Reducing the computational requirements of adaptive equalization in underwater acoustic communications," Proc. *Oceans '95*. San Diego, CA, pp. 1405-1410, Oct. 1995.

[7] S. Haykin, Adaptive Filter Theory, New Jersey: Prentice Hall. 1986.

[8] P. Bragard and G. Jourdain, "A fast self-optimized algorithm for non-stationary identification: application to underwater equalization," *Proc. ICASSP '90*, pp. 1425-1428.

[9] B. Geller, V.Capellano, J.-M.Brossier, A.Essebar and G.Jourdain, "Equalizer for video rate transmission in multipath underwater communications," *IEEE J.Oceanic Eng.*, vol. 21, pp.150-155, Apr. 1996.

[10] V. Capellano, Gerard Loubet and G. Jourdain, "Adaptive multichannel equalizer for underwater communications," Proc. *Oceans '96*, pp. 994-999, Ft. Lauderdale, FL, Oct. 1996.

[11] B. Woodward and H.Sari, "Digital underwater voice communications," *IEEE J. Oceanic Eng.* vol. 21, pp.181-192, Apr. 1996.

[12] G. S. Howe et al., "Sub-sea remote communications utilising an adaptive receiving beamformer for multipath suppression," in Proc. *OCEANS'94*, pp. I.313-I.316, Brest, France, Sept. 1994.

[13] A. Benveniste, M. Metivier, and P. Priouret, Adaptive Algorithms and Stochastic Approximations. Berlin: Springer Verlag. 1990.

[14] E. Eleftheriou and D Falconer, "Tracking properties and steady-state performance of RLS adaptive filter algorithms," *IEEE Trans. ASSP*, Vol ASSP-34, No. 5, pp 1097-1109, Oct. 1986.

APPENDIX A

Improved Doppler Tracking and Correction For Underwater Acoustic Communications

IMPROVED DOPPLER TRACKING AND CORRECTION FOR UNDERWATER ACOUSTIC COMMUNICATIONS

*Mark Johnson, Lee Freitag and Milica Stojanovic**

Woods Hole Oceanographic Institution, Woods Hole, Massachusetts 02543
*Northeastern University, Boston, Massachusetts 02115

ABSTRACT

The performance of coherent acoustic communication systems involving moving platforms (e.g., underwater vehicles and ships) is adversely effected by Doppler shift resulting from relative motion of the transmitter and receiver. This paper presents a series of innovations which, together, dramatically improve the response to Doppler shift of a widely-used adaptive receiver algorithm. The innovations include a frequency-shift estimator, time-scale interpolator and robust phase-locked loop (PLL). These techniques reduce the computational load of the coherent equalizer and provide accurate Doppler tracking. Results from at-sea testing are presented to illustrate the performance of the combined algorithm.

1. INTRODUCTION

The feasibility of bandwidth-efficient underwater acoustic communications has been recently established [1]. There is now a growing interest in the development of more sophisticated signal processing algorithms which will enable communication in adverse conditions of multipath and rapid phase variation. These development efforts aim to improve existing algorithms in a manner which will make them suitable for emerging applications. One such application is communication with an autonomous underwater vehicle (AUV), a task seriously complicated by large and variable Doppler shifts.

The adaptive decision feedback equalizer (DFE), in the kernel of many coherent communications receivers [2], is capable of decoding signals with moderate levels of Doppler shift. However, this requires the equalizer to rapidly adjust feedforward parameter phase, which is both computationally intensive and introduces adaptation noise [3]. An improved DFE algorithm containing an embedded phase-locked-loop (PLL) to remove carrier shift due to Doppler has been in use [1,4], but its performance has been unsatisfactory under realistic field conditions.

This work was sponsored in part by the Office of Naval Research under contracts N-00014-96-1-1198 and N00014-94-1-0714.

To alleviate this problem, we investigate in this paper an alternative method for phase synchronization and equalization in the presence of large Doppler shifts. The proposed receiver algorithm performs signal detection in two steps. In the first step, the motion-induced Doppler shift is coarsely estimated and removed from the received signal. In the second step, residual Doppler shift is eliminated in the equalizer by the PLL which is modified from the original presented in [1]. We show that by performing carrier phase synchronization in a theoretically suboptimal way, the system is more robust to the choice of tracking parameters and has improved stability properties. Such features are desirable when the Doppler shift is subject to rapid variations as is the case with AUV communications.

The paper is organized as follows. In Section 2 the Doppler estimator and pre-processor is presented. In Section 3 details and performance trade-offs of the PLL within the equalizer are discussed. Finally, in section 4 the performance of the algorithm with experimental data is examined.

2. DOPPLER ESTIMATION AND COMPENSATION

Figure 1 shows the Doppler pre-processor portion of the receiver. First the frequency shift is estimated from the training (i.e., *a priori* known) data at the start of each received packet using an ambiguity function method. To minimize computation, the ambiguity function is computed across the range of Doppler shifts $\omega_{min} < \omega < \omega_{max}$ expected in a given application and at a resolution somewhat finer than the Doppler spread. The estimate is found by computing

$$\hat{\omega}_d = \max_{\omega_{min} < \omega < \omega_{max}} \sum_{k=0}^{n-1} e^{j\omega k} d_k x_k \qquad (1)$$

where x is the received data sequence and d is the length n training sequence. The performance of the estimator is proportional to both n and the signal to noise ratio. The Cramer-Rao lower bound on the variance of the estimator is given by

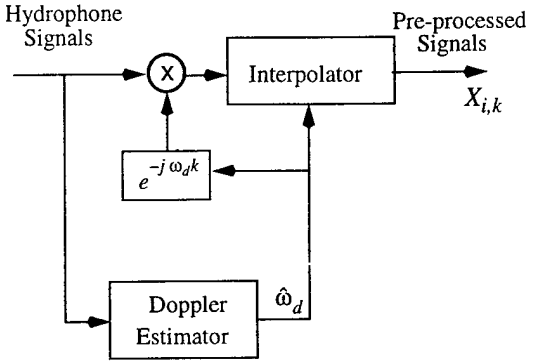

Figure 1: Doppler pre-processor which estimates frequency shift of the incoming data packet, removes that offset, then interpolates to shift the time scale of the data.

$$E\left[\left|\hat{\omega}_d - \omega_d\right|^2\right] \geq \frac{1}{\eta\tau^2} \qquad (2)$$

where τ is the observation time and η is the output SNR after matched-filtering [7]. The sequence length n is large (several hundred symbols) and data rates are modest (1000-5000 symbols per second), thus yielding very accurate Doppler estimates. Fig. 3 shows results of using the estimator during at-sea trials and demonstrates the variability of Doppler under realistic field conditions.

Using the coarse Doppler estimate, the centre frequency of each received signal is shifted and the time-scale is then adjusted using an interpolator. As the change in sampling-rate is typically very small (<1%), a polyphase interpolator provides an efficient implementation. In this method, the received signal is processed by a sequence of filters with increasing (or decreasing, depending on the sign of the Doppler shift) time delay, selected from a pre-computed filter bank.

The computational load of the interpolator is proportional to the filter length and may be considerable if low spectral distortion is required over the full input frequency range. In coherent acoustic communications, a fractional-spaced equalizer is used to provide accurate timing alignment and so the input sampling rate to the equalizer is usually twice that indicated by the Nyquist criterion [2]. This implies that the interpolator need only perform well in the half band from 0 to 1/4 of the input sampling rate. The interpolator filter bank can then be generated using a least-squares technique to minimize spectral distortion in the band of interest. The resulting interpolator offers satisfactory performance with extremely short filters. For example, with length-3 filters, the signal-to-distortion ratio is >20dB over the half band (a level of performance sufficient for QPSK signals), and with length-5 filters, 40dB is attained.

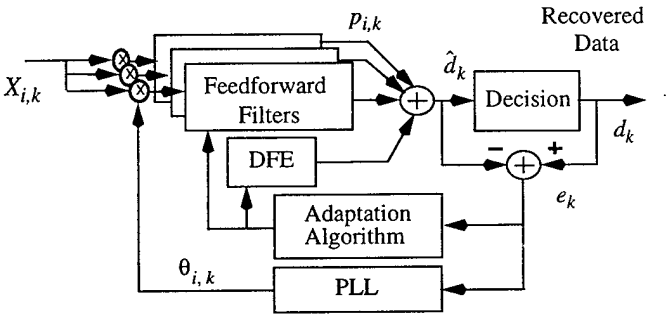

Figure 2: DFE equalizer with fine-scale phase shift correction in advance of the individual channel feedforward filters. Feedforward and feedback outputs are combined and the error term is generated by a decision device. The RLS algorithm is used for adaptation.

3. Phase-Locked Loop

In phase-coherent underwater communications, an adaptive equalizer is essential to overcome signal distortion due to multipath propagation and fading. In the equalizer structure of Fig. 2, the adaptive feedforward sections combine the Doppler-corrected input signals so as to maximize the signal-to-noise ratio of the direct arriving sound and remove inter-symbol-interference (ISI) due to dispersion. The DFE section is tasked with removing ISI due to multipath propagation. The feedforward and DFE sections are jointly adapted so as to minimize the mean-square-error (MSE) in the output symbol sequence. As noted above, the equalizer is itself able to correct for moderate levels of Doppler shift by continuously varying the phase of the feedforward filters. However this is a computationally expensive approach as the equalizer is forced to update at a much higher rate than would otherwise be necessary to

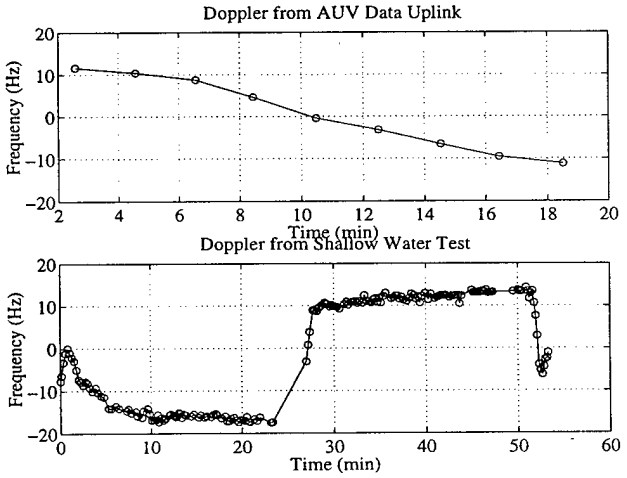

Figure 3: Doppler estimates obtained using the method of equation (1) with actual field data. Top: Doppler shift experienced when a AUV passes a stationary vessel. Bottom: Doppler shift over time for a shallow water experiment with two moving vessels.

track changes in the acoustic environment. A technique overcoming this limitation, proposed in [1], is to embed a multi-channel PLL in the equalizer designed to correct phase shifts in the output of the feedforward channels due to Doppler shift. The PLL is adjusted jointly with the equalizer using a gradient estimate of the form

$$g_{i,k} = \mathrm{Im}\{p_{i,k}(e_k + p_{i,k})^*\} \tag{3}$$

where i and k are the channel and time index, respectively, $p_{i,k}$ is the output of the ith feedforward section and e_k is the symbol error. The gradient estimate is combined with a second order filter to form a servo control loop.

Although shown to work in some situations, the method of [1] suffers from slow oscillatory convergence and, in certain cases, instability. This is a result of positive error feedback in the equalizer adaptation whenever phase correction term has a negative real part (e.g., between $\pi/2$ and π). Positive feedback is a well known cause of divergence in RLS adaptations [5]. The problem is eliminated by reversing the order of the phase correction and feedforward terms as shown in Fig. 2. Such re-ordering involves a slow-convergence assumption on the equalizer and PLL which appears to be fulfilled in all practical situations.

Unfortunately, a new problem is introduced by the re-ordering: the loop gain of the PLL is now dependant on the instantaneous value of the feedforward coefficients. This results in unpredictable PLL convergence rate and difficulty in setting the PLL tracking gain parameter. In order to overcome this problem, a modified phase gradient is proposed which is sensitive only to the phase of the product in (3)

$$g_{i,k} = \mathrm{Im}\{\log(p_{i,k}(e_k + p_{i,k})^*)\}. \tag{4}$$

Use of this gradient, although theoretically sub-optimal, has been found to give very similar converged MSE performance to (3). However, the transient response of the PLL using (4) is more predictable and can be set independently of the equalizer coefficients.

The resulting equalizer equations for m input channels are given below. Fractional spacing is accommodated by assuming that r new observations are made on each channel at each time step k.

Step 1: update regressor vector with new observations $X_{i,k}$ using PLL output $\theta_{i,k}$

$$\Psi_{i,k} = \begin{bmatrix} e^{-j\theta_{i,k}} X_{i,k} \\ \Psi_{i,k-1}(1 \ldots n_i - r) \end{bmatrix} \quad \text{for} \quad i = 1 \ldots m \tag{5}$$

where n_i is the length of the ith feedforward section.

Step 2: compute feedforward section output using coefficient vector $A_{i,k}$

$$p_{i,k} = A_{i,k}^H \Psi_{i,k} \tag{6}$$

Step 3: compute feedback section output using the coefficient vector B_k applied over the vector of previous outputs D_{k-1}

$$t_k = B_k^H D_{k-1} \tag{7}$$

Step 4: compute symbol prediction $\hat{d}_k$ and error e_k

$$\hat{d}_k = t_k + \sum_{i=1}^{m} p_{i,k} \tag{8}$$

$$e_k = d_k - \hat{d}_k \tag{9}$$

where d_k is the nearest valid symbol to $\hat{d}_k$.

Step 5: update phase-locked loop

$$\theta_{i,k} = G\left(q^{-1}\right)\left(\mathrm{Im}\{\log(p_{i,k}(e_k + p_{i,k})^*)\}\right) \tag{10}$$

using a second order filter with gain g

$$G\left(q^{-1}\right) = \frac{g\left(1.1 - q^{-1}\right)}{1 - 2q^{-1} + q^{-2}}. \tag{11}$$

Step 6: update equalizer coefficient matrix $\mathbf{R}$

$$\mathbf{R}_{k+1} = \mathbf{R}_k + \lambda \begin{bmatrix} \Psi_{1,k} \\ \cdots \\ \Psi_{m,k} \\ D_{k-1} \end{bmatrix} \begin{bmatrix} \Psi_{1,k}^H & \cdots & D_{k-1}^H \end{bmatrix} \tag{12}$$

$$\begin{bmatrix} A_{1,k+1} \\ \cdots \\ A_{m,k+1} \\ B_{k+1} \end{bmatrix} = \begin{bmatrix} A_{1,k} \\ \cdots \\ A_{m,k} \\ B_k \end{bmatrix} + \mathbf{R}_{k+1}^{-1} \begin{bmatrix} \Psi_{1,k} \\ \cdots \\ \Psi_{m,k} \\ D_{k-1} \end{bmatrix} \tag{13}$$

where $\lambda < 1$ is the forgetting factor. Note that (12) and (13) are performed implicitly using a square-root RLS algorithm [2].

The two key user-selected parameters in the equalizer are the PLL gain, g, and the RLS forgetting factor, λ, both of which control the responsiveness of the equalizer to changing conditions. There is an essential redundancy in these parameters due to the fact that both the RLS-adaptation and the PLL can track phase changes. This redundancy gives rise to an ill-conditioned transient response in the equalizer whereby residual Doppler shift is compensated by a combination of adaptation and PLL action. As we are concerned only with the quality of the symbol estimate rather than the instantaneous values of the equalizer parameters, this ambiguity is not a problem except for the higher-than-necessary computation load it can cause. In practice, choosing the PLL tracking rate to be significantly higher than the equalizer tracking rate (parameterized by $1 - \lambda$, eliminates much of the competition between the

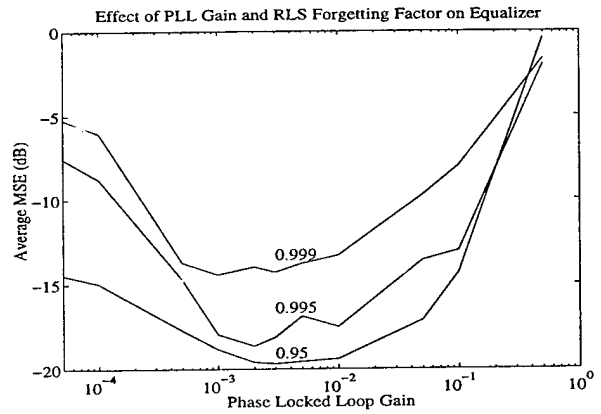

Figure 4: Performance of the equalizer with varying PLL gain and RLS forgetting factor, λ. The time constant of equalizer memory is $1/1-\lambda$ symbols. This in-water data set was Doppler compensated but has a time-varying Doppler shift.

two systems. The use of MSE thresholding in the RLS update [6] also forces the PLL to dominate in tracking Doppler shift.

4. Experimental Results

The performance of the new receiver in tracking and correcting Doppler shift has been evaluated with data from moving platforms at relative speeds of up to 6 knots. Evaluating the system with this data provides information on setting key parameters for the equalizer.

In Fig. 4 MSE as a function of the PLL and equalizer tracking parameters is shown. This is for a single QPSK packet at 1250 symbols/sec. Over a large range of RLS forgetting factors almost a decade of PLL gain adjustment is possible with little ill effect. However, as gain is decreased, the forgetting factor must be reduced to allow the equalizer to compensate phase not removed by the slowly-responding PLL. At high gain, overall equalizer performance suffers as phase noise introduced by the over-energetic PLL is added to each output symbol.

Fig. 5 shows the difference in the computation requirement per symbol needed to successfully decode a set of 21 consecutive packets spanning 0 to 15 Hz both with and without Doppler pre-compensation. The savings in computations comes about through two mechanisms. The first is that the number of feedforward parameters, which are required to act as interpolating filters, is reduced. The second savings arises because the equalizer is only updated when the MSE exceeds a certain threshold [6]. With pre-processing, fewer updates are needed to track the residual phase and time-scales changes in the signal. The computational requirement for an RLS update is $O(n^2)$, where n is the total number of parameters, and thus any reduction in parameter count or update rate is significant for real-time operation.

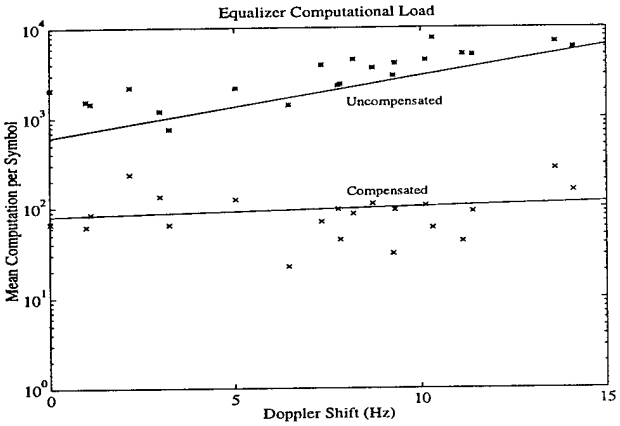

Figure 5: Comparison of computation burden while processing a variety of data packets over a range of Dopper shifts (the first 10 minutes from Fig. 3). The carrier is 12.5 kHz and the data rate is 1250 symbols/sec.

Conclusion

Doppler pre-processing is made possible by a sequence of known symbols in the data which allow accurate estimation of the carrier frequency shift. Interpolation via polyphase filters provides a computationally efficient method for adjusting the time scale of the data and this pre-processing removes the requirement for long feedforward sections which would otherwise be needed as interpolators. The total savings is very large, a factor of 50 in RLS update cost, for Doppler shifts greater than 0.1 percent. Additionally, the overall performance of the equalizer is expanded because parameterization and tracking concentrate on removing ISI, not frequency offsets and time shifts.

References

[1] M. Stojanovic, J. Catipovic, J. Proakis, "Phase coherent digital communications for underwater acoustic channels", *IEEE J. Oceanic Eng.*, Vol. OE-16, pp. 100-111, Jan. 1994.

[2] J. Proakis, *Digital Communications*, 2nd ed., New York: McGraw-Hill, 1989.

[3] B. Widrow et al. "Stationary and non-stationary learning characteristics of the LMS adaptive filter", *Proc. IEEE*, Vol. 64, No. 8, August 1976, pp.1151-1162.

[4] M. Stojanovic, J. Catipovic, and J. Proakis, "Adaptive multichannel combining and equalization for underwater acoustic communications," *J. Acoust. Soc. Am.*, Vol. 94, No. 3, Pt. 1, Sept. 1993.

[5] B.D.O. Anderson, C.R. Johnson, "Exponential convergence of adaptive identification and control algorithms", *Automatica*, Vol. 18, No. 1, 1982, pp. 1-13.

[6] Mark Johnson, D. Brady, M. Grund, "Reducing the computational requirements of adaptive equalization in underwater acoustic communications", *OCEANS'95*, San Diego, Sept. 1995.

[7] W. S. Burdic, *Underwater Acoustic System Analysis*, Englewood Cliffs: Prentice-Hall, 1984.

APPENDIX B

Efficient Equalizer Update Algorithms for Acoustic Communication Channels of Varying Complexity

Efficient Equalizer Update Algorithms for Acoustic Communication Channels of Varying Complexity

Lee Freitag, Mark Johnson and Milica Stojanovic*

Woods Hole Oceanographic Institution, Woods Hole, MA
*Northeastern University, Boston MA

Abstract—**Underwater acoustic communication channels vary from stationary with sparse arrivals to rapidly varying and fully reverberant. A receiver structure capable of operating over this wide range of characteristics has evolved in recent years and consists of a fractionally-spaced multi-channel combiner, a sparse DFE, and an embedded PLL. At the computational heart of this receiver is an adaptation algorithm, used to update the various equalizer parameters. The adaptation algorithm may use one of the standard strategies such as adaptive step-size LMS, RLS, adaptive memory RLS, or a hybrid of these. The choice of algorithm involves trade-offs between training time, tracking-rate, operating SNR, and computational requirements of the receiver. To maximize the receiver throughput, we wish to select the least computational algorithm for which the error-rate is still acceptable and, given the volatility of the underwater channel, this choice should be made for each received packet. In this paper, we compare the performance of several LMS and RLS adaptation algorithms over a range of real acoustic data. We show that the computationally-efficient adaptive step-size LMS performs well for many channel classes, but that the faster tracking of RLS is essential for some complex non-stationary channels. The results provide a first step towards the automatic selection of adaptation algorithm, as would be required in a fully autonomous receiver.**

I. Introduction

Compared to many other communication media, underwater acoustic channels are generally bandlimited and so involve relatively low data rates. Despite this, the channel distortions commonly encountered require complex signal processing in the receiver, resulting in high computational loads and the need for power-hungry, high-speed DSP hardware. Consequently, the design of a computationally-efficient receiver is crucial for practical implementations.

The problem of reducing receiver complexity may be addressed on two levels: (i) in the design of an efficient parametric receiver structure, and (ii) in the choice of an efficient algorithm to adapt the receiver parameters. The receiver structure considered here has been developed over several years and consists of a multichannel DFE with fractionally-spaced feedforward filters and an embedded phase-locked loop [1][2]. This receiver is able to decode coherently-modulated data in difficult acoustic environments at a wide range of frequencies and data rates [1][3]. A number of modifications have been proposed to further reduce the receiver computational load, including an improved phase-locked loop, sparse DFE parameterization, and efficient resampling to compensate for Doppler-induced time dilation [3].

The receiver may use any of a number of adaptive algorithms for adjusting its parameters, although typically an algorithm from the LMS or RLS families is selected [4]. LMS-based algorithms have been preferred in several recent studies due to their low computational complexity, which is linear in the total number of parameters, N [5][6][7]. However, in a fully-developed multipath environment, N may be very large (more than 100) and this can lead to an unacceptably long convergence time [4]. In addition, the performance of LMS is very sensitive to the choice of step-size. To overcome this latter problem, self-optimized LMS algorithms [5][8] have been used at some cost in complexity.

RLS algorithms, including the square-root version which is well suited for single-precision implementations [9], have better convergence properties than LMS but much higher computational complexity. Indeed, the quadratic complexity of standard RLS [4] is infeasible for real-time applications when N is much larger than 100. This has led to interest in the family of 'fast' RLS algorithms having linear complexity. Unfortunately, such algorithms typically suffer from high numerical sensitivity and have reduced flexibility of application, relying upon a shifting property in their input signals [10]. Although a numerically stable fast RLS algorithm [10][11] has been used for multichannel equalizer tests in off-line processing [2], it has an awkward trade-off between tracking rate and numerical stability which tends to limit its application.

The preceeding comments underscore an inevitable trade-off: adaptation algorithms with low computation rates are less able to decode highly distorted data than their more complex counterparts, and so in the rapidly-varying underwater channel, the best choice of adaptive algorithm, from the combined viewpoint of computational efficiency and accurate decoding, may change on a packet-by-packet basis. The aim of this paper is to compare the performance of several LMS and RLS algorithms with real acoustic data in an effort to establish under what conditions LMS may be acceptable.

The paper is organized as follows: in Section II the structure of the DFE and the different update algorithms are intro-

This work was supported in part by the Defense Advanced Research Project Agency under contract MDA972-95-0006 and by the Office of Naval Research under N00014-95-1-0496.

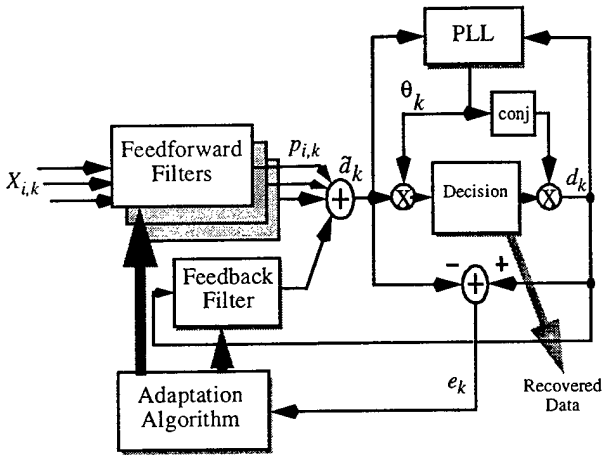

Figure 1. The DFE with m input hydrophones, m fractionally-spaced (r samples per symbol) feedforward filters and single phase-locked loop implemented at the summing junction of the feedforward and feedback sections. The error signal e_k is provided to an adaptive filter algorithm of choice which updates the weights as well as maintains state as required.

duced and issues which influence the selection of a particular algorithm are discussed. In Section III the performance of the different update algorithms are compared using data from at-sea tests, both easy and challenging, and conclusions drawn about both efficiency as well as overall robustness.

II. Equalizer Structure and Update Algorithms

The equalizer algorithm, shown in Fig. 1, contains a DFE augmented by fractionally-spaced (r samples per symbol) input filters for each of m channels and coupled with a phase-locked loop operating to track the joint phase estimate. With this structure, the regressor vector, used to adapt the equalizer parameters, consists of r new observations for each channel at each iteration which are added to a total of n_i parameters for each feedforward filter. The regressor vector is thus:

$$\Phi_k = \begin{bmatrix} X_{1,k} \\ \vdots \\ X_{1,k-\frac{n_1}{r}} \\ \vdots \\ X_{m,k} \\ \vdots \\ X_{m,k-\frac{n_m}{r}} \\ D_{k-1} \end{bmatrix} \tag{1}$$

where $X_{i,k}$ is an r-vector of observations at time k for the ith hydrophone, pre-processed so as to remove a majority of the effects of Doppler shift and converted to baseband. D_{k-1} is the m-vector of previously decoded symbols used for decision feedback.

The estimate, $\tilde{a}_k$, of the next data symbol, d_k, is computed using the current parameter vector:

$$\tilde{a}_k = \Theta_k^H \Phi_k \tag{2}$$

where Θ_k is the vector of length:

$$N = p + \sum_{i=1}^{m} n_i \tag{3}$$

collecting all of the adaptive parameters in the equalizer. The transmitted symbol is deduced from $\tilde{a}_k$ by:

$$d_k = e^{j\theta_k} Decision\{e^{-j\theta_k}\tilde{a}_k\} . \tag{4}$$

The error is then computed as:

$$e_k = d_k - \tilde{a}_k \tag{5}$$

and the PLL updated as

$$\theta_k = G(q^{-1})\left(\mathrm{Im}\{\log(d_k^* \tilde{a}_k)\}\right) \tag{6}$$

where:

$$G(q^{-1}) = \frac{g(1.1 - q^{-1})}{1 - 2q^{-1} + q^{-2}} . \tag{7}$$

Lastly, the equalizer parameters are updated with the adaptive algorithm:

$$\Theta_{k+1} = Update(\Theta_k, \Phi_k, e_k) . \tag{8}$$

This adaptation step dominates the computational cost of the receiver and also determines many of its performance properties. Of particular concern are the effect of update algorithm choice on the convergence-rate and operating SNR of the receiver, and these are discussed in turn in the following.

The convergence rate of the update algorithm is a function of the number of parameters, N, and the richness of the input signals. For reasons of bandwidth efficiency, it is desirable to have rapid initial convergence of the equalizer. However this is difficult to achieve with LMS algorithms if N is large or if there is substantial spectral disparity in the received signals (e.g., due to multipath arrivals). Because of its second-order structure, the convergence rate of RLS is much less sensitive to the input signal quality and N although numerical stability can become an issue in extreme cases.

The minimum SNR for which decoding is possible at the receiver is determined in part by the misadjustment noise of the update algorithm. Misadjustment is due to the tracking behavior of the algorithm and there is an unavoidable trade-off between fast tracking and misadjustment noise. For a giv-

en tracking rate, the misadjustment tends to increase linearly with N and so becomes an important limiting factor where the channel complexity is high. In such cases, adaptive step-size algorithms which dynamically adjust their tracking rate so as to minimize the MSE, offer an important advantage.

In the following section, we consider an LMS and an RLS implementation of (8) and compare the resulting performance.

III. Comparison of LMS and RLS Algorithms

It is difficult to fairly compare algorithms that can optimally adjust their tracking parameters with those that are fixed, so in order to compare RLS and LMS the adaptive versions of each are used. While the adaptive step-size LMS has been presented in [5] for use in underwater acoustic communication, the adaptive-memory RLS has not yet appeared in the literature for this application.

A. The Adaptive Algorithms

The LMS algorithm with adaptive step size requires computing the time-varying step-size μ_k and the gradient estimate Y_k. These are given by [8]:

$$Y_{k+1} = (I - \mu_k \Phi_k \Phi_k^H) Y_k + \Phi_k e_k^* \quad \text{and} \tag{9}$$

$$\mu_{k+1} = \mu_k + \alpha Re(Y_k^H \Phi_k e_k) \tag{10}$$

where α is a small learning-rate variable. As written, the update Y_{k+1} is $O(n^2)$ so it is re-ordered as

$$Y_{k+1} = Y_k - \mu_k \Phi_k (\Phi_k^H Y_k) + \Phi_k e^*{}_k. \tag{11}$$

To demonstrate how the optimal step-size changes over time, an hour of transmissions between two slowly moving vessels in 100-200 m deep water was processed with this algorithm. The acoustic channel varies from extremely simple, with high SNR and only a few arrivals, to low SNR with a long and sparse response. The optimal step size (Fig. 4) varies by more than 4 over the test. At the beginning it is approximately 0.02 however, as the range increased and more parameters are needed by the equalizer (and SNR decreases), μ drops below 0.005.

The RLS algorithm with adaptive memory [8] is based on the direct form, version II [4]. The algorithm requires additional computations for the derivative of the inverse correlation matrix:

$$\mathbf{S}_{k+1} = \frac{1}{\lambda_k}(I - K\Theta_k^H)\,\mathbf{S}_k(I - \Theta_k K^H) + \frac{1}{\lambda_k}(KK^H - R) \tag{12}$$

the gradient:

$$\Psi_{k+1} = (I - K\Theta_k^H)\,\Psi_k + \mathbf{S}_k \Phi_k e_k \tag{13}$$

and the time-varying forgetting-factor:

$$\lambda_{k+1} = \lambda_k + \alpha Re(\Psi_k^H \Phi_k e^*{}_k) \tag{14}$$

where α is the learning coefficient and the forgetting factor is limited over the range $1_{\min} < \lambda_k < \lambda_{\max}$.

While this algorithm is computationally intensive, it is a useful tool for benchmarking RLS-based equalizers and it provides the best ultimate performance over a variety of channels.

One of the main drawbacks of the LMS algorithm is the potentially long convergence time. However, it is possible to utilize a simple hybrid of RLS and LMS to speed training and yet track efficiently. To accomplish this the RLS (direct form) is used for training and then the update task is taken over by the LMS algorithm. Since the LMS load is quite small in

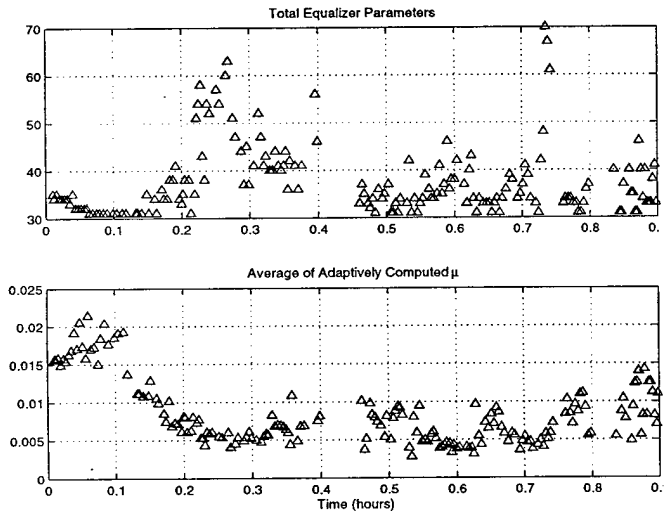

Fig. 2. LMS step-size determined adaptively by the self-tuning algorithm of equations 9-10 for one hour of moving source-receiver testing in coastal waters.

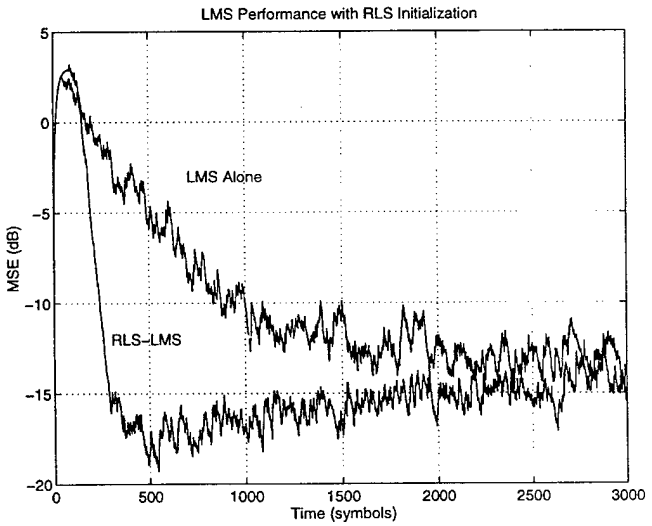

Fig. 3. Performance of the RLS-LMS algorithm. The training period of LMS is almost 2000 symbols while the RLS convergences in about 500. The transition from RLS to LMS occurs at the 500 symbol point.

comparison to RLS, both are run in parallel during the training period with the RLS-computed weights provided as input to the adaptive LMS. Fig. 3 shows an example of this, the LMS by itself has a long convergence time, but when provided with the RLS parameters after training is capable of tracking for the remainder of the packet.

B. Experimental Results

The algorithms are compared using data that represent a number of different realistic underwater acoustic channels. In all cases the signals are 1250 symbol per second QPSK centered at 2.25 kHz. To detect the start of a packet a 13-chip Barker code is sent prior to the data. The Barker code provides approximately 11 dB of gain after match-filtering for the impulse response plots shown in this section. The transmitted signals were received on vertical arrays and processed using one to fifteen hydrophones to demonstrate the performance provided by multi-channel receivers. The deep-water data is from an array with 6.6 m element spacing, the shallow water tests were conducted using 1 m spaced hydrophones.

The first case is from a 40-km deep-water test with the array located at 750 m. As may be seen in Fig. 4-A, the channel response consists of two closely-spaced rays which span only a few symbols. The overall performance of both update algorithms is essentially identical for one to fifteen channels.

The second example (Fig. 4-B) is taken at 30 km range in 200 m water on the New England continental shelf. The impulse response spans about 60 msec (75 symbols) and while there are a number of ways to parameterize this channel (selection of feedforward and feedback tap lengths), here the width of the feedforward section is fixed at 12 taps per channel and 50 parameters are used for the feedback filter. The adaptive RLS enjoys a clear performance advantage here, up to 5 dB, depending on the total number of channels used. In this case the LMS has both a longer training period and the total misadjustment error after training is larger than that of the RLS. However, despite this difference the LMS algorithm easily provides adequate MSE for QPSK and 8-PSK data transmission.

The third case (Fig. 5) is taken in an upward sloping acoustic environment but at a range of about 20 km. The impulse response has doubled in length and is now strongly acausal. For each hydrophone channel 40 feedforward taps are used and the number of feedback taps is fixed at 80. The large number of resulting parameters (up to 700) makes adaptive-memory RLS computationally prohibitive and the direct form RLS with constant forgetting-factor is used instead. Despite the complex impulse response and deep spectral nulls the LMS algorithm is fully capable of providing parameter updates which adequately track this channel and provide low error-rate communication. As the number of parameters grows the performance difference between the two algorithms narrows, and ultimately LMS surpasses RLS by about one-half dB. It must be borne in mind that this difference results from use of fixed-memory RLS: for optimal performance the forgetting factor should have been reduced slightly as the number of parameters was increased.

While the adaptive LMS algorithm provides good performance in the three cases discussed above, when the channel is changing rapidly the tracking ability of the adaptive LMS may not be sufficient to maintain the MSE needed for proper DFE operation. An example of this is shown in Fig. 6 where a channel complexity similar to that of Fig. 5 is combined with time-varying effects. The LMS MSE is too high for error-free operation and the DFE diverges when the channel begins to change rapidly. In contrast, the additional 2 dB of performance gain available with the RLS (operated here with fixed forgetting factor) allows error-free operation.

IV. Conclusion

The performance of LMS and RLS adaptation algorithms in a multichannel DFE has been compared using at-sea data. The data provided a range of underwater acoustic channels from relatively benign to extremely challenging. For simple channels, for which few adaptive parameters are required, LMS and RLS update algorithms show very similar results. However, as channel complexity grows, the performance of LMS degrades with respect to RLS, most notably in terms of convergence rate but also due to the increased misadjustment noise of LMS. The slow convergence rate of LMS can be overcome for stable moderate complexity channels by using RLS during the training period and then switching to LMS for the remainder of the packet.

When the total number of parameters increases to many hundreds, as required in the most complex channels, the performance of LMS is only acceptable where the channel is relatively stationary. In such cases, LMS offers reasonable performance at a tremendous computational savings over the direct form RLS. However, in cases where high complexity is combined with nonstationarity, the extra tracking capability of RLS can make the difference between success and failure for the DFE. Thus, unfortunately, some of the most complex channels require the more computationally intensive update algorithm.

References

[1] M. Stojanovic, J. Catipovic and J. Proakis, "Adaptive multichannel combining and equalization for underwater acoustic communications," *J. Acoust. Soc. Am.*, Vol. 94, (3), Pt.1, pp. 1621-1631. Sept. 1993.

[2] M. Stojanovic, J. Catipovic and J. Proakis, "Phase coherent digital communications for underwater acoustic channels", *IEEE J. Oceanic Eng.*, Vol. OE-16, pp 100-111, Jan. 1994.

[3] M. Johnson, L. Freitag and M. Stojanovic, "Improved Doppler Tracking and Correction for Underwater Acoustic Communication," in Proc. *ICASSP'97*, vol 1, pp.575-578, Munich, Germany, April, 1997.

[4] S. Haykin, Adaptive Filter Theory, New Jersey: Prentice Hall. 1986.

[5] B. Geller, V.Capellano, J.-M.Brossier, A.Essebar and G.Jourdain, "Equalizer for video rate transmission in multipath underwater communications," *IEEE J.Oceanic Eng.*, vol. 21, pp.150-155, Apr. 1996.

[6] B. Woodward and H.Sari, "Digital underwater voice communications," *IEEE J. Oceanic Eng.* vol. 21, pp.181-192, Apr. 1996.

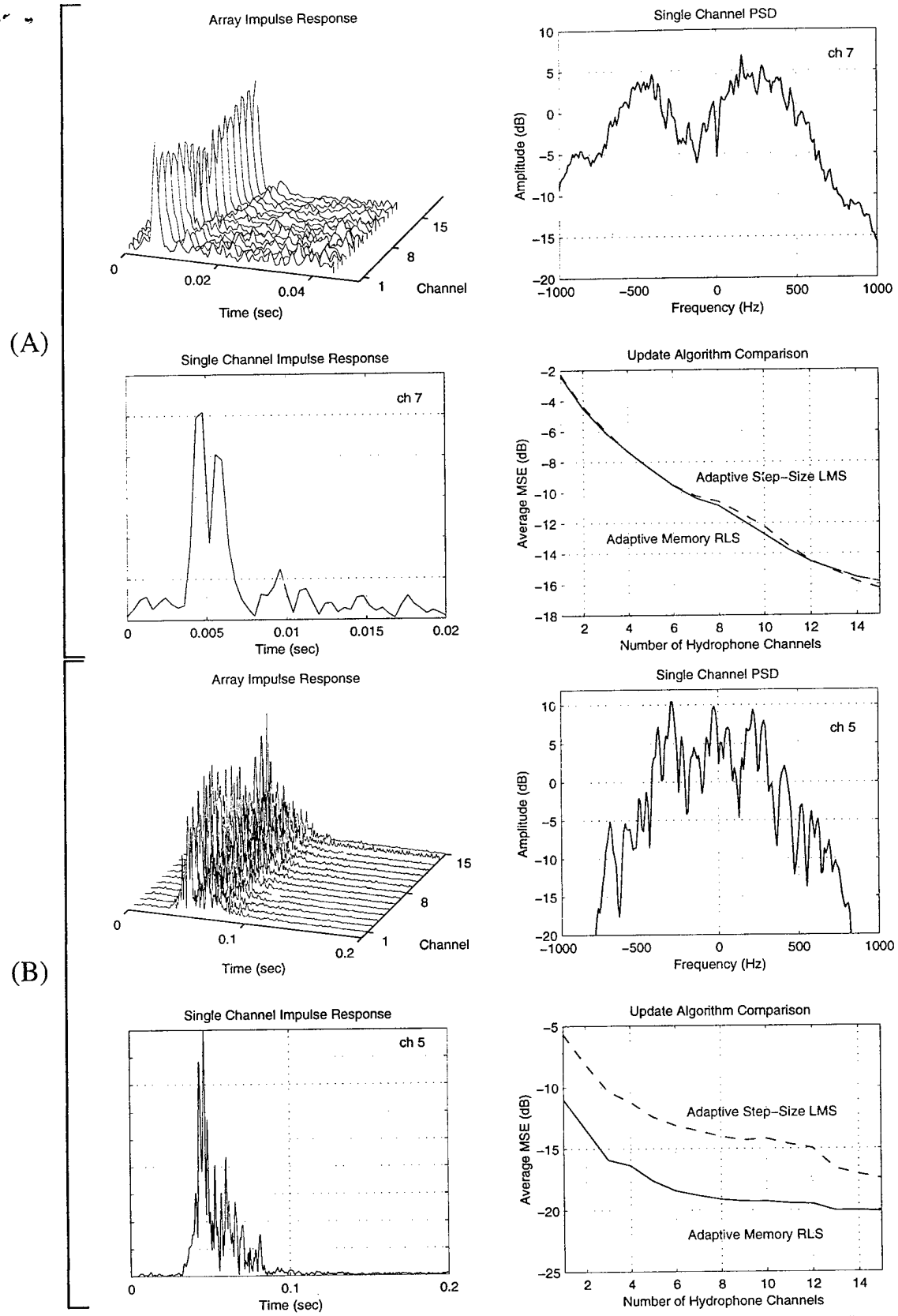

Fig. 4. Performance of the adaptive memory RLS and the adaptive step-size LMS algorithms under two different channel conditions. (A) The 40 km deep-ocean channel with a simple impulse response. For each feedforward filter 6 taps are used and the number of feedback parameters is fixed at three. Thus as the number of channels increases from 1 to 15 the total number of parameters goes from 9 to 93 and performance for both algorithms increases as well. (B) The 30 km shallow water (200 m) New England continental shelf. In this example 12 feedforward filter taps are used per channel and the number of feedback parameters is fixed at 50. Here the parameter range is 62 to 230. Here the high SNR and deep spectral nulls provide the RLS with a large performance advantage.

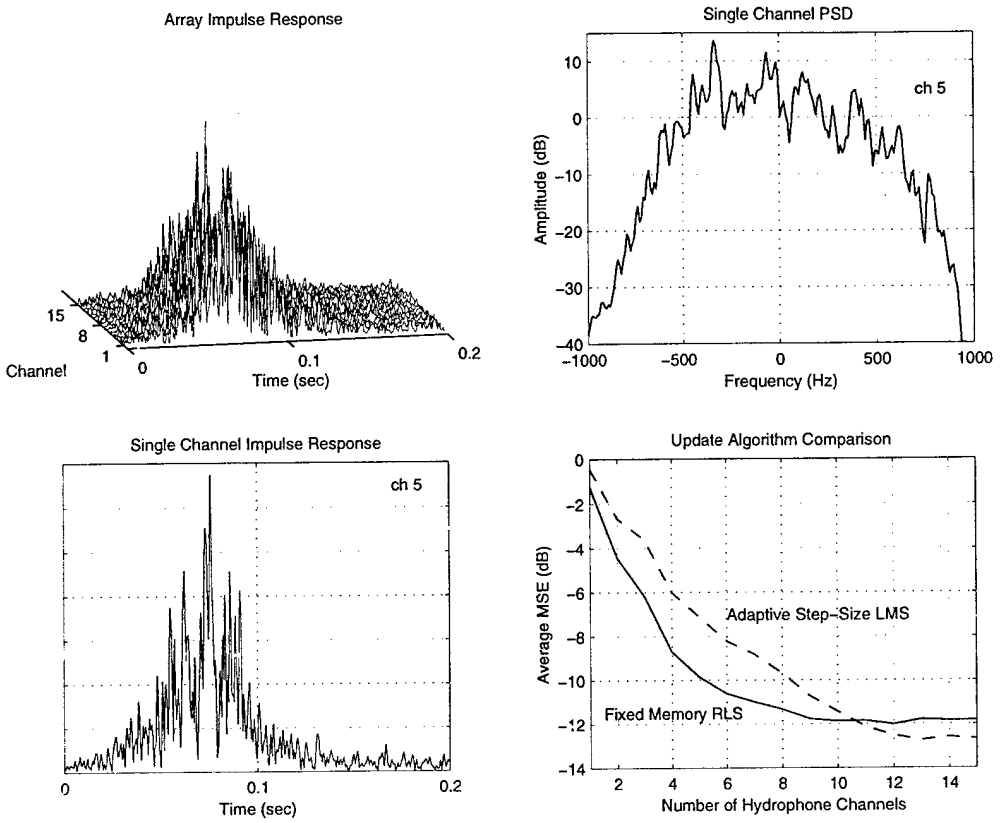

Fig. 5. Algorithm performance at about 20 km in upward sloping bathymetry. The total impulse response spans about 125 symbols (250 T/2 taps). Here 40 feedforward filter taps are used per channel and the number of feedback parameters is fixed at 80. The parameter range shown in the lower left is thus 100 to 700 as the number of channels is increased from 1 to 15. The large number of parameters precludes the use of the adaptive memory RLS and the fixed version is used instead. Thus as the number of parameters increases and the forgetting factor should have been decreased, the performance difference narrows and finally the adaptive LMS offers improved performance. This illustrates the difficulty of maximizing performance with constant adaptation rates.

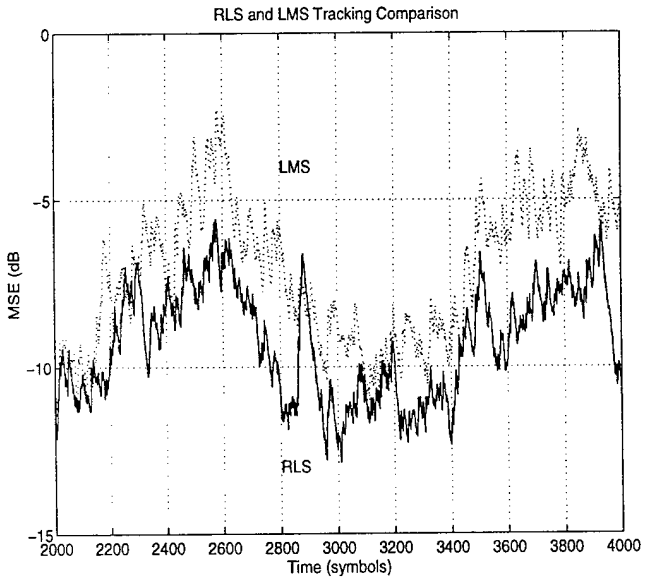

Fig. 6. Tracking performance of RLS and adaptive step-size LMS with correct symbols always fed back for the DFE. The mean-square error of the LMS is not sufficient for DFE operation with QPSK data and when operated in decision-directed mode it will diverge. In contrast, the RLS tracks the channel changes and no errors occur in decision-directed mode.

[7] G. S. Howe et al., "Sub-sea remote communications utilising an adaptive receiving beamformer for multipath suppression," in Proc. *OCEANS'94*, pp. I.313-I.316, Brest, France, Sept. 1994.

[8] A. Benveniste, M. Metivier, and P. Priouret, Adaptive Algorithms and Stochastic Approximations. Berlin: Springer Verlag. 1990.

[9] F. Hsu, "Square root Kalman filtering for high-speed data received over fading dispersive HF channels," *IEEE Trans. Inform. Theory*, Vol. IT-28, pp. 753-763, Sept. 1982.

[10] D. Slock and T.Kailath, "Numerically stable fast transversal filters for recursive least squares adaptive filtering," *IEEE Trans. Sig. Proc.*, vol. SP-39, pp. 92-114, Jan. 1991.

[11] D. Slock, L.Chisci, H.Lev-Ari and T.Kailath, "Modular and numerically stable fast transversal filters for multichannel and multiexperiment RLS," *IEEE Trans. Sig. Proc.*, Vol. 40, pp.784-802, Apr. 1992..